International Journal of Innovative Engineering Applications

A REVIEW AND EVALUATION STUDY OF MAXIMUM POWER POINT TRACKING TECHNIQUES FOR PV SYSTEMS

Fuad Alhaj Omar[*1] iD

[1]*Department of Electric and Energy, Zonguldak Bülent Ecevit University, Turkey.*

Abstract

Original scientific paper

The issue of improving the efficiency and effectiveness of PV (Photovoltaic) systems remains a concern for researchers and manufacturers who aim to make these systems cost-effective, thereby encouraging their wider adoption. To achieve this goal, increasing the efficiency of the PV generation system by implementing the Maximum Power Point Tracking (MPPT) system has been proposed. Enhancing the energy output from the PV system is considered a crucial aspect of improving efficiency, as it will lead to increased revenue. Consequently, the cost of the generated energy is reduced, approaching that of energy produced by conventional systems based on fossil fuels. This review paper discusses conventional MPPT techniques designed to extract the maximum available power from PV panels operating under uniform environmental conditions. Subsequently, it highlights why these techniques often fail to perform adequately under partial shading conditions. Following this, modern MPPT techniques explicitly designed to operate under non-uniform and partial shading conditions are analyzed.

Keywords: MPPT; photovoltaic system; partial shading conditions; hot spot phenomena; global tracking.

PV SİSTEMLERDE KULLANILAN MAKSİMUM GÜÇ NOKTASI İZLEME TEKNİKLERİNİN İNCELENMESİ VE DEĞERLENDİRİLMESİ

Özet

Orijinal bilimsel makale

PV sistemlerinin verimliliğini ve etkinliğini artırma konusu, bu sistemleri maliyet etkin hale getirmeyi ve böylece daha geniş çapta benimsenmesini teşvik etmeyi amaçlayan araştırmacılar ve üreticiler için bir endişe kaynağı olmaya devam etmektedir. Bu amaca ulaşmak için maksimum güç noktası izleme (MPPT) sistemi kullanılarak PV üretim sisteminin verimliliğinin artırılması önerilmiştir. PV sisteminden üretilen enerjiyi artırmak, gelirleri artıracağı için verimliliği artırmada önemli bir unsur olarak kabul edilir. Sonuç olarak, üretilen enerjinin maliyeti düşmekte, bu da fosil yakıta dayalı geleneksel sistemlerden üretilen enerjinin maliyetine yaklaşmasına neden olmaktadır. Bu makale, tek tip çevresel koşullar altında çalışan PV panellerinden maksimum kullanılabilir gücü çıkarmak için tasarlanmış geleneksel MPPT tekniklerini tartışmaktadır. Daha sonra bu tekniklerin kısmi gölgeleme koşulları altında yeterli performans gösterememesinin nedeni vurgulanmıştır. Bunu takiben, kısmi gölgeleme koşulları altında çalışmak üzere tasarlanmış modern MPPT teknikleri analiz edilir.

Anahtar Kelimeler: MPPT; fotovoltaik sistem; kısmi gölgeleme koşulları; sıcak nokta fenomeni; global izleme.

1 Introduction

Recently, the importance of renewable energy has reached an unmatched height as a result of fossil fuel depletion. Among all the renewable energy resources the PV systems have received the most attention due to several merits, for instance, environmental friendliness, availability, low maintenance, and a longer lifespan, (typically more than 20 years) [1]. These advantages have contributed to the rapid development of PV systems worldwide in comparison to other types of renewable energy sources [2, 3]. The strong dependence of PV systems upon the atmospheric conditions makes extracting the maximum available power from its nonlinear characteristics more difficult [4], (see Figure 1).

During the past several years, with the intention of handling this issue and enhancing the efficiency of PV systems and extracting as much power as possible from PV modules, many MPPT strategies have been proposed and established [6, 7]. Proposed MPPT techniques differ in several aspects such as simplicity, efficiency, sensor requirements, cost, hardware implementation,

---

convergence speed and other aspects. Each algorithm has its own features and applications. Since one is suitable for a specific application and not suitable for another, they can be classified into two categories: the conventional MPPT algorithms and new MPPT optimization algorithms. However, if employing a simpler and less expensive algorithm can yield similar even superior results, it does not seem sensible to adopt a more expensive or more sophisticated method. This is the reason why some of the proposed algorithms are not preferred in PV system realizations. In the following sections, an overview of the many proposed MPPT algorithms is presented.
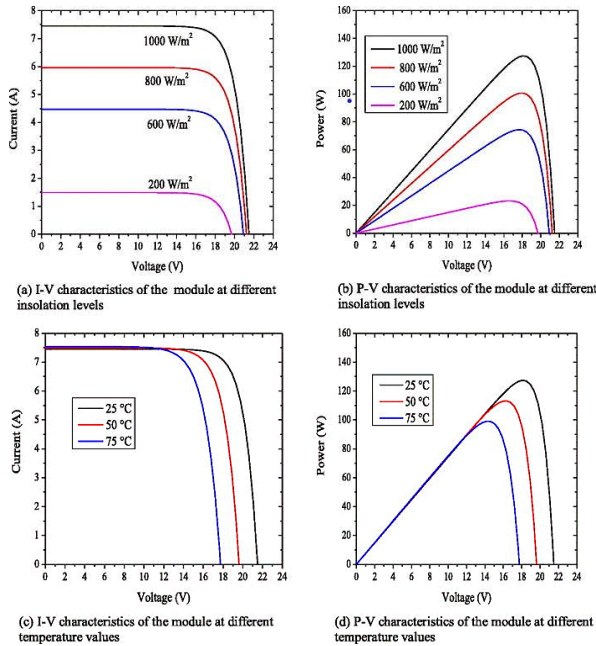

Figure 1. Characteristics of the PV module under different irradiance levels and temperatures [5].

2 Conventional MPPT Techniques

2.1 Constant Voltage (CV) Algorithm

This algorithm is considered one of the simplest and fastest MPPT techniques. By matching the measured solar module voltage V_PV to a constant reference voltage equal to the V_MPP , the operating point is kept near MPP [8]. In this technique, only one voltage sensor is employed to measure the solar module voltage V_PV and compare it with the reference voltage V_MPP , from which the corresponding duty cycle of the DC-DC converter is set up [9], as shown in Figure 2.
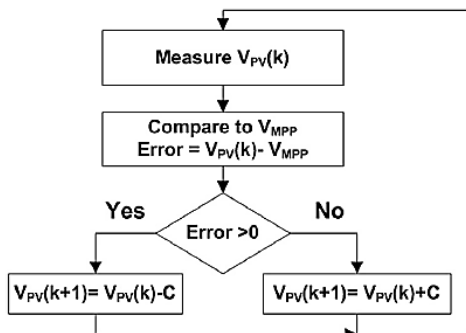

Figure 2. Constant voltage algorithm flowchart [10].

The main drawback of this technique is that it neglects the effects of ambient temperature and irradiance level on the solar module; therefore, the operating point does not exactly match the MPP. Generally, this technique is often integrated with other MPPT techniques to obtain high accuracy and enhance the efficiency of the PV system [10].

2.2 Open Circuit Voltage Method

This method relies on the linearly proportional relationship between open-circuit voltage V_OC and the PV module output voltage at MPP. The relationship is given in equation (1), where K_1 is a constant that relying on the fill factor FF, photocell features, and atmospheric conditions [11].

$$V_{MPP} \cong K_1 . V_{OC} \qquad (1)$$

The value of K_1 has to be determined beforehand by measuring the values (V_{OC}, V_{MPP}) for the PV module being used under various insolation and temperature levels and it is reported to be in the range between 0.71 and 0.8. Once the K_1 is known, the system is momentarily interrupted to measure V_{OC}. Subsequently, the V_{MPP} can be computed using the equation (1) and MPP will be updated [10]. This method can be achieved with the flowchart shown in Figure 3. Since the equation (1) is only an approximation, the operating point technically is never matching to the MPP and this incurs power loss. Even though this method is not a true MPPT technique, it is inexpensive and simple to implement as it is not necessary to use microcontrollers [12].
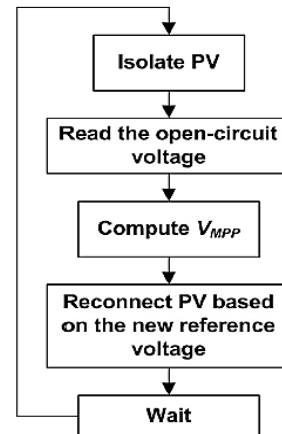

Figure 3. Open circuit voltage algorithm flowchart [10].

2.3 Short Circuit Current Method

Just like in the open-circuit voltage method, the short-circuit current method is based on the observed fact that, under fluctuating weather conditions, the PV module current at MPP (I_{MPP}) is nearly linearly related to the short-circuit current (I_{SC}) of the same PV module, as illustrated in equation (2) [12, 13].

$$I_{MPP} \cong K_2 . I_{SC} \qquad (2)$$

Where, K_2 is a proportionality constant depending largely on the photocell features, atmospheric conditions, and the fill factor FF. Similar to the previous method, K_2 has to be previously determined by performing a scan on the PV module being used under various insolation and temperature levels. However, the constant K_2 is between (0.78 and 0.92). In order to measure (I_{SC}) during the operation, a switch and a current sensor must be added to the system [14]. This will increase the complexity and cost.

If the DC-DC boost converter is used, then the transistor in the converter can be delegated to short the PV module [15]. Hence, the benefits and drawbacks of this method are similar to those of the open-circuit voltage method. The flow chart of this method is shown in Figure 4.
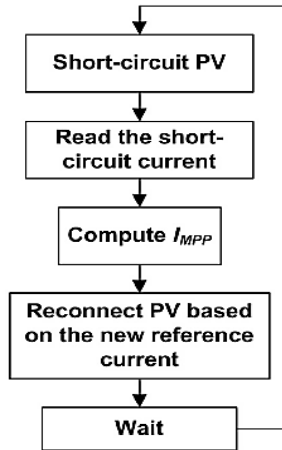
Figure 4. Short circuit current algorithm flowchart [10].

2.4 Open Circuit Voltage Pilot PV Cell Method

This method was proposed to eliminate the defects resulting from the interrupting process occurring in the open-circuit voltage method during the measurement of V_{OC} [10]. Wherein a pilot solar cell; which is electrically isolated from the rest of the PV module; is used to measure the value of open circuit-voltage V_{OC}, then according to the previous equation (1), the corresponding maximum voltage value V_{MPP} is determined. Under partial shading conditions, this technique suffers from inaccuracy. This results in a mismatch between the V_{MPP} of the pilot solar cell and the actual value of the used solar module [16].

2.5 Feedback Voltage or Current Method

Similar to the constant voltage method, in this technique, a feedback control loop is used to deliver the voltage (current) extracted from the solar module to a certain level. The control process is performed by using the error; the difference between the reference voltage and the solar module voltage (current); with a view to calibrating the duty cycle of the DC-DC converter [17], as shown in Figure 5.

The algorithm can bring the operating point of the system near to the actual MPP with a slight iteration. Although the algorithm has the advantages of high convergence speed, simplicity, and ease of implementation, it fails to find the real MPP under partial shading conditions [10].
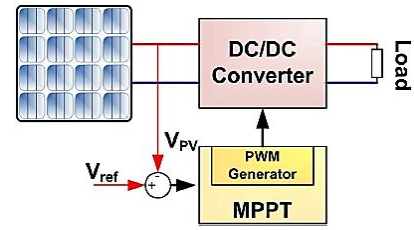
Figure 5. Voltage-feedback with PWM modulation [10].

2.6 P-N Junction Drop Voltage Tracking Method

This method is based on the physical fact that the thermal characteristics of the solar cell are similar to the p-n junction diode. Consequently, low-cost p-n junction diodes are utilized to produce the reference voltage of the solar module, where they are integrated into the reverse side of the solar panel. Therefore, the surface temperature changes in the atmosphere will be detected by the diodes, causing a change in the forward voltage across the p-n junction diodes [18]. Figure 6 shows the control circuit used in this method, where the input voltage of the pulse width modulator is given as follows:

$$dV_R = K_2(V_{PV} - V_{ref}) = K_2(V_{PV} - K_1 V_d) \qquad (3)$$

where, V_{PV} is the output voltage of the PV module, V_{ref} is the reference voltage, V_d is the voltage across the p-n junction diodes, K_1 is the gain of the amplifier Amp1 and K_2 is the gain of the amplifier Amp2.
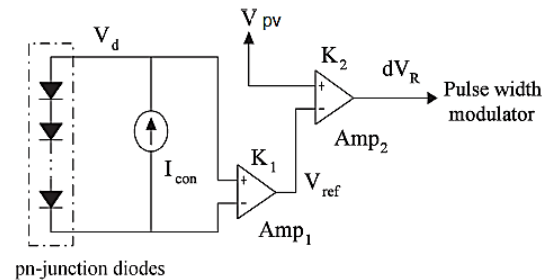
Figure 6. Control-circuit configuration of the P-N junction drop voltage tracking method [10].

2.7 Look-up Table Method

For the proposed MPPT technique, a look-up data table of all possible atmospheric conditions is formed in advance to be compared with actual atmospheric conditions. Then, depending on the control system, the saved values are compared with the actual values of the temperature and insolation. According to the comparison result, a duty cycle corresponding to the MPP is generated. The comparison process is carried out every cycle to ensure that the operating point is at the highest available power MPP [19, 20]. This method is predetermined based on practical tests under different atmospheric conditions. The controller used should contain a memory with a large enough storage capacity for storing the available input data.

2.8 Load Current or Load Voltage Maximization

When connecting a power converter to a PV module, maximizing the extracted power from the PV module leads to maximizing the output power of the converter. In contrast, maximizing the output power of the converter leads to a super extracting power from the PV module, on the assumption that energy losses in the converter are zero. It should be noted that most loads are either resistance, voltage-source, current source, or integration of all these kinds [21], as illustrated in Figure 7. In voltage source type load, in order to obtain the maximum output power, the load current should be maximized. For other kinds of loads, the output current or output voltage can be utilized to maximize the output power. In this technique, only one sensor is required. Therefore, maximizing the output power for all types of load can be carried out by maximizing either the output current or output voltage. In this technique, to control the power converter and adjust the operating point of the PV module to keep it near the MPP, a feedback loop is used. According to the assumption that the power converter losses are zero, operating cannot be achieved exactly at the MPP, and this is one of the drawbacks of this method [22, 23].
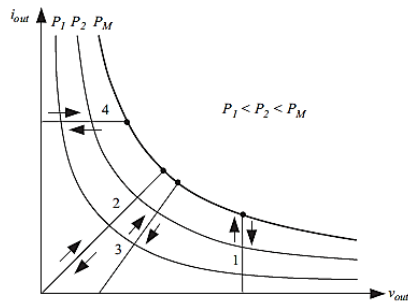

Figure 7. Load types: 1-voltage-source, 2-resistive, 3-resistive and voltage-source, 4-current-source [21].

2.9 Only Current Photovoltaic Method

In this algorithm, the output power can be maximized depending on the PV current [24]. In this system, a battery is connected to the PV module across a DC-DC converter; thus, regardless of the value of duty cycle D, the output voltage (battery voltage V_{bat}) will be constant. The block diagram of this technique is shown in Figure 8.
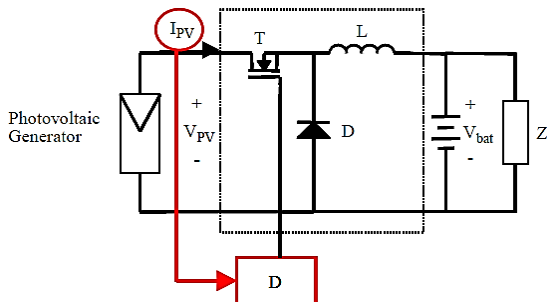

Figure 8. Block diagram of the only-current method [24].

In the case of buck converter, the output voltage (battery voltage) can be given as shown:

$$V_{bat} = \frac{T_{on}}{T} V_{PV} = D.V_{PV} \tag{4}$$

where, T is the period time and T_{on} is the the duration of the controlled switch is ON.

The input power of the converter can be determined as:

$$P_{in} = V_{PV}.I_{PV} = V_{bat}.\frac{I_{PV}}{D} = V_{bat}.P_{BUCK}^* \tag{5}$$

Where

$$P_{BUCK}^* = \frac{I_{PV}}{D} \tag{6}$$

According to the algorithm of Figure 9, four cases can be presented in Table 1.

$$\Delta P^* = P^*(t + \Delta t) - P^* \tag{7}$$

$$\Delta D = D(t + \Delta t) - D(t) \tag{8}$$

It can be seen from the algorithm that, after computing the present and the past data of P_{BUCK}^*, and based on the equation (8), the controller decides whether to reduce or enhance the duty-cycle ratio. This tracking process will be repeated until the MPP is reached [10].

The advantage of this method is the PV module current is the only control variable. Moreover, this method has a good efficiency even under different atmospheric conditions and can be implemented with any type of DC-DC converter not just with a buck converter [23].
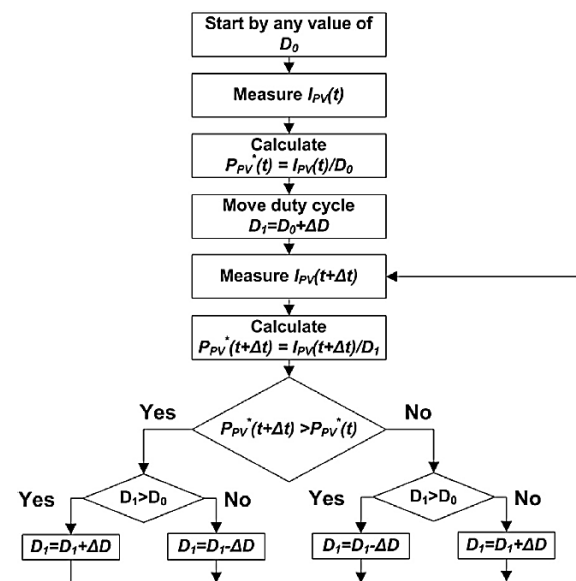

Figure 9. Flowchart of the only-current photovoltaic method [10].

Table 1. Decision the change in the duty cycle after measuring and storing the past and the present information [23].

Case	ΔP	ΔD	Following step
1	>0	>0	+ΔD1
2	>0	<0	−ΔD1
3	<0	>0	−ΔD2
4	<0	<0	+ΔD2

2.10 PV Output Senseless (POS) Control Technique

In the POS MPPT technique, the load voltage is omitted, and the load current is the only significant component. As known, the load power is related to the harvested power from the PV module, and multiplying the voltage with the current is equal to a load power. Therefore, increasing the load current leads to an increase in the load power and from there increases the generated power by the PV module. This simple algorithm (shown in Figure 10) can be applied to all PV generation systems. The POS MPPT technique finds the MPP by comparing the duty cycle with the load current value [25, 26]. The details of the POS algorithm are presented in Table 2 and Figure 11.
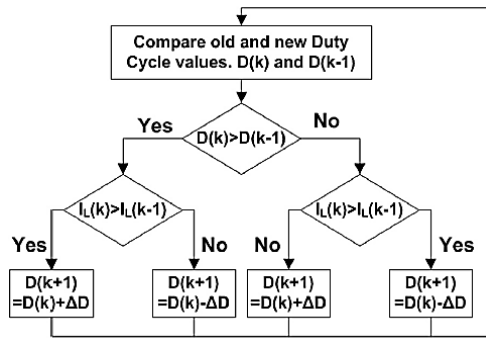

Figure 10. Flowchart of the POS MPPT technique [10].

Table 2. A conceptual explanation of POS MPPT technique [25].

Track	Duty ratio	Current (I)	Δ Duty ratio
1 ($V_0 \rightarrow V_1$)	(−)	(+)	(−)
2 ($V_1 \rightarrow V_2$)	(−)	(−)	(+)
3 ($V_2 \rightarrow V_3$)	(+)	(+)	(+)
4 ($V_3 \rightarrow V_1$)	(+)	(−)	(−)

From Figure 11: in track 1, if the value of the duty cycle decreases, the generated voltage by the PV module moves from V_0 to V_1, and the generated power increases from P_0 to P_1. In track 2, the value of the duty cycle will decrease, the generated voltage moves from V_1 to V_2 and the generated power decreases from P_1 to P_2. In track 3, if the duty cycle increases, the generated voltage decreases from V_2 to V_3 and the generated power increases from P_2 to P_3. In track 4, the duty cycle will increase, the generated voltage decreases from V_3 to V_1 and the generated power decreases from P_3 to P_1. Therefore, the duty cycle will decrease, and all of these steps will be repeated until POS MPPT reaches the MPP [25].
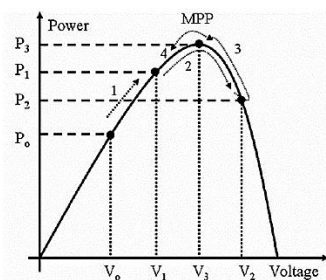

Figure 11. The explanation of POS MPPT technique [25].

This technique is very useful in extracting maximum power from the PV module with the feedback of only the load current. Moreover, it can be operated effectively on a large scale PV generation system.

2.11 Perturb and Observe (P&O) Method

Among all the papers reviewed, significant attention was directed towards the Perturb and Observe (P&O) method, which is considered one of the most commonly used techniques for tracking the Maximum Power Point (MPP). This method operates on the principle of perturbing the duty cycle value and observing the resulting power extracted from the PV module [27]. In each cycle of the P&O method, the control unit calculates the power generated by the PV module, then adjusts the duty cycle and monitors the power variation. If the extracted power increases, the subsequent perturbation is made in the same direction until the MPP is reached. Conversely, if the extracted power decreases, the next perturbation is reversed [28]. The basic principle of the P & O algorithm is summed up in Table 3 and shown in Figure 12. The block diagram of this technique is illustrated in Figure 13.

Table 3. A Summary of the P&O method.

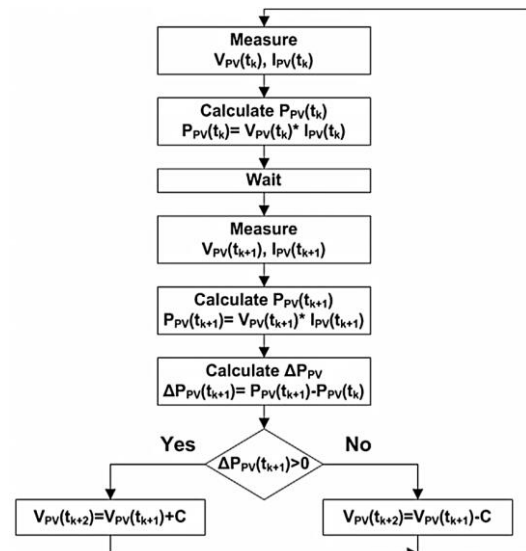| Perturbation	Change in Power	Next Perturbation
Positive	Positive	Positive
Positive	Negative	Negative
Negative	Positive	Negative
Negative	Negative	Positive

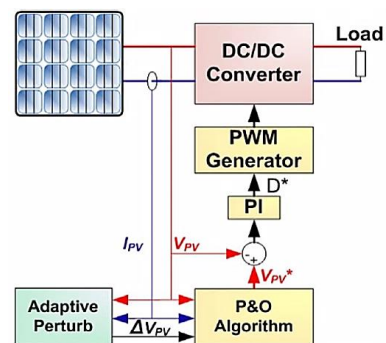**Figure 12.** The flowchart of the P&O algorithm [10].

Figure 13. The block diagram of the P&O method [10].

After reaching the MPP, the operating point starts oscillating around the MPP leading to loss of power. With the aim of reducing the steady-state oscillation, the perturbation step size must be minimized. However, small step values cause a low speed of tracking the MPP. Using a two-stage algorithm that exhibits a large step value in the first stage and a low step value in the later stage is considered a solution to the problem between the faster tracking and steady-state oscillations [10].

However, this method suffers another drawback. This method fails under a swift change in atmospheric conditions as shown in Figure 14. Assuming that the operating point is A, if the atmospheric conditions stay nearly constant, the next perturbation will move the operating point to B and, due to reduction in power, the following perturbation will be reversed. However, within one iteration, if the atmospheric conditions change and displace the power curve from P_1 to P_2, the operating point will shift from A to C. This will appear as an increase in power and the next perturbation will be kept in the same direction resulting in loss of power [21, 29].
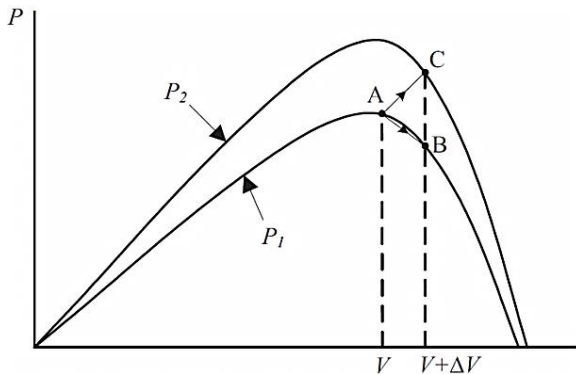

Figure 14. Divergence of the P&O from MPP [21].

The vital advantage of this method is that the characteristics of the PV module are not required, and it can be implemented for all types of PV modules. Two sensors, one for voltage and the other for current, are used to compute the extracted power from the PV module. DSPs or microprocessors are used in this technique.

2.12 Three-Point Weight Comparison Method

In the P&O algorithm, in order to monitor the change in power and determine whether to increase or decrease the subsequent duty cycle, the values of power at the current operating point and the subsequent operating point are compared. Additionally, the operating point in the P&O algorithm oscillates around the MPP resulting in a loss of the extracted power from the PV module. Therefore, to avoid the loss of power under rapid atmospheric condition changes, the three-point weight comparison algorithm was proposed [10, 30]. This algorithm runs periodically by perturbing the duty cycle which is applied on the DC-DC converter and comparing the PV module output power on three points on the P-V curve. The three points are as follows:

- A: The current operating point.
- B: perturbed positively from point A.
- C: perturbed negatively from point A.

To reach the MPP, nine possible states should be carried out in the control unit as depicted in Figure 15. The procedures of the algorithm are as follows:

1) If the power at point B is greater than or equal to the power at point A the status is assigned positively weighted; otherwise if the power at point B is smaller, the status is negatively weighted.
2) If the power at point C is greater than or equal to the power at point A, the status is negatively weighted; otherwise, the status is positively weighted.
3) According to the comparison of the three points, if two cases are negatively weighted, the duty cycle will be decreased in the next iteration; otherwise when two cases are positively weighted, the duty cycle will be increased. In other cases, if one is negatively weighted and the other is positively weighted, the MPP is reached and the duty cycle should not be changed. A flowchart of this algorithm is shown in Figure 16 [31].
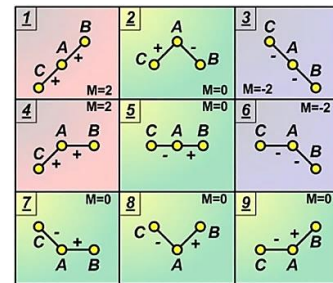

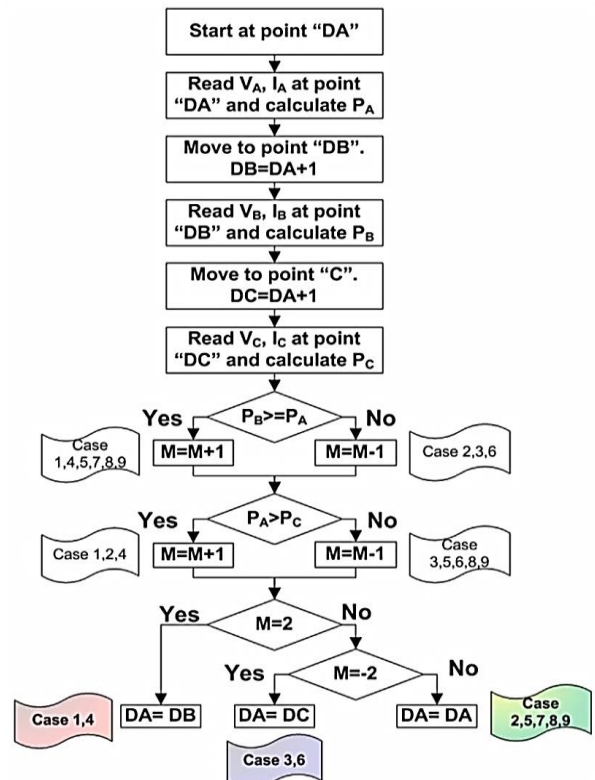**Figure 15.** Possible states of the three-point weight comparison algorithm [10].

Figure 16. The flowchart of the three-point weight comparison algorithm [10].

2.13 On-line MPP search algorithm

In this algorithm, shown in Figure 17, the reference maximum power is determined and compared with the current power [10]. The difference between the two values is called the maximum power error. If the maximum power error is zero, the MPP is reached [32].

At first, the reference values of the maximum power, P_{ref}, and reference current, I_{ref}, are set to zero, and the reference voltage, V_{ref}, is equated to the open-circuit voltage V_{oc} of the PV module. At each iteration, the deference, P_{error}, between the reference power, P_{ref}, and the current operating power, P_{actual}, are computed and compared with the assumed error, $P_{tolerance}$. If the deference, P_{error}, is smaller than the assumed error, $P_{tolerance}$, the initial values, P_{ref}, I_{ref} and V_{ref} are reassigned by, $P_{actual,ref}$, $I_{acutual,ref}$ and $V_{acutual,ref}$, respectively, and used as reference values for the next iteration. If the deference, P_{error}, is greater than the assumed error, $P_{tolerance}$, a new MPP will be searched by the algorithm. If the current operating power, P_{actual}, is greater than the reference power, P_{ref}, then the operating values, P_{actual}, I_{actual}, and V_{actual} are reassigned by, $P_{actual,ref}$, $I_{acutual,ref}$ and $V_{acutual,ref}$, respectively, and used as reference values for the next iteration. If the operating power, P_{actual}, is smaller than the reference power, P_{ref}, then the operating current, I_{actual}, and voltage, V_{actual}, will be compared with I_{ref} and V_{ref}, respectively. If the operating current I_{actual} is greater than I_{ref} or the operating voltage is smaller than V_{ref}, then the operating values, P_{actual}, I_{actual}, and V_{actual} are reassigned by, $P_{actual,ref}$, $I_{acutual,ref}$ and $V_{acutual,ref}$, respectively [33].

The success of this algorithm in capturing the MPP is related to the operating power of the load P_{actual}. If P_{actual} is small, the algorithm will fail to find the MPP. To avoid that, extra loads must be connected to increase the operating power so MPP can be reached. This algorithm can find the new MPP under rapidly changing atmospheric conditions.
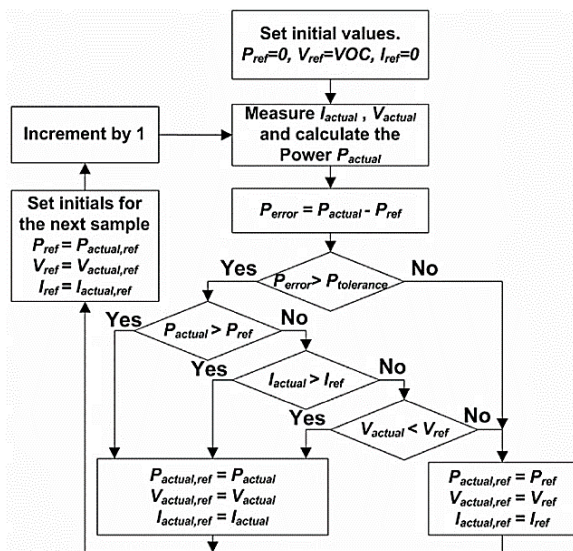

Figure 17. The flowchart of the on-line MPP search algorithm [10].

2.14 DC-Link Capacitor Droop Control

This method is particularly developed to be used with a PV system that is connected in parallel with a DC to AC inverter [10], as illustrated in Figure 18. Assuming that a boost converter is connected between the PV module and the inverter, the duty cycle on an ideal boost converter is given as:

$$D = 1 - \frac{V_{PV}}{V_{link}} \tag{9}$$

Where:
V_{PV} is the input voltage of the boost converter.

V_{link} is the output voltage of the boost converter, which is the voltage across the DC-link.

The control process in this MPPT method is based on discerning the voltage drop across the DC-link voltage V_{link} [34]. If the V_{link} is kept constant alongside increasing the current passing across the AC inverter, this leads to an increase in the power coming from the boost converter and consequently increases the extracted power from the PV module. When the required power by the inverter surpasses the maximum available power from the PV module, the DC-link voltage V_{link} begins dropping. Right before that point, the system works at the MPP and the current control command I_{peak} of the AC inverter is at its maximum value. The ac system line current is fed back to prevent V_{link} from drooping and the duty cycle is optimized to fetch I_{peak} to its maximum value; consequently, MPPT is achieved. The main drawback of this technique is the low response. This is because its response relies directly on the response of the dc voltage control loop of the AC inverter [35, 36].
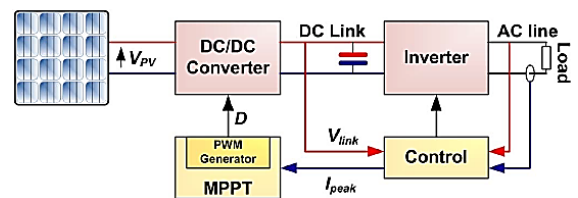
Figure 18. Topology of a DC-link capacitor droop control [10].

2.15 MPPT with a Variable Inductor

In this technique, a buck converter is used to make the load resistance equal to the resistance of the PV panel [37]. In this case, according to the max power transfer theorem, the maximum available power will be transferred from the PV panel to the load. The load resistance R_L is matched to the PV panel resistance R_{PV} by controlling the duty cycle D, R_{PV} is given as:

$$R_{PV} = \frac{V_{PV}}{I_{PV}} = \frac{V_L}{I_L D^2} = \frac{R_L}{D^2} \tag{10}$$

To satisfy the last equation, the buck converter must operate in the continuous current mode (CCM). During CCM the minimum inductance in a buck converter is given as:

$$L_{min} = \frac{R_L.(1-D)}{2.f_s} \qquad (11)$$

where, f_s is the switching frequency.

The relation between the input and the output current of a buck converter is given as:

$$I_{PV} = D.I_L \qquad (12)$$

By combining the last equations (10), (11) and (12), the relationship between L_{min} and the I_{PV} is given as:

$$L_{min} = \frac{D.(1-D).V_{PV}}{2.f_s.I_L} = \frac{D^2.(1-D).V_{PV}}{2.f_s.I_{PV}} \qquad (13)$$

By assuming that the voltage does not change over the full range of the solar irradiance, the minimum inductance, which keeps the buck converter in the CMM, becomes related to the load current and the duty cycle or the PV current and the duty cycle [38].

2.16 Current Sweep Method

This method depends on determining the derivative of the PV array output power with regards to the array output current while the array output current is adapted as a decaying exponential sweep function [10]. In this method, a sweep waveform is used in order to obtain the I-V characteristic curve of the PV array, and this curve will be updated at fixed time periods [39]. Then, from the I-V characteristic curve, the V_{MPP} can be computed during the same periods. The current sweep waveform can be calibrated as a predefined function of time.

$$I_{PV}(t) = f(t) \qquad (14)$$

The function $f(t)$ selected for the sweep waveform is directly proportional to its derivative as follows:

$$f(t) = k.\frac{df(t)}{dt} \qquad (15)$$

where, k is a proportionality constant. Along this sweep waveform the PV array power is given by:

$$P_{PV}(t) = V_{PV}(t).I_{PV}(t) = V_{PV}(t).f(t) \qquad (16)$$

As known at MPP the derivative of $P_{PV}(t)$ is zero.

$$\frac{dP_{PV}(t)}{dt} = V_{PV}(t).\frac{df(t)}{dt} + f(t).\frac{dV_{PV}(t)}{dt} = 0 \qquad (17)$$

Substituting $f(t)$ in the last equation gives:

$$\frac{dP_{PV}(t)}{dt} = \left[V_{PV}(t) + k.\frac{dV_{PV}(t)}{dt}\right].\frac{df(t)}{dt} = \qquad (18)$$

The solution of the differential equation in (15) is given as:

$$f(t) = C.e^{t/k} \qquad (19)$$

where, C is the arbitrary constant which is selected to be equal to the maximum current of the PV array I_{max}. If k is selected to be negative, that leads to a decrease in exponential function with time constant $\tau = k$.

$$f(t) = I_{max}.e^{-t/\tau} \qquad (20)$$

By using some current discharging through a capacitor, the current in (20) can be easily obtained. By dividing both sides of the (18) equation on $\frac{df(t)}{dt}$ with $f(t) = I_{PV}(t)$:

$$\frac{dP_{PV}(t)}{df(t)} = \frac{dP_{PV}(t)}{dI_{PV}(t)} = V_{PV}(t) + k.\frac{dV_{PV}(t)}{dt} = 0 \qquad (21)$$

Once V_{MPP} is calculated after the current sweep, the equation (21) is used to verify whether the MPP has been reached. This technique needs about 50 ms to reach MPP, resulting in some power loss. Therefore, this MPPT method is suitable if the tracking unit consumes power lower than the increase in power that it can extract from the PV array [40].

2.17 Incremental Conductance (IC) Technique

This technique depends on calculating the differential of the PV power to PV voltage to determine the location of the operating point [41], where the differential is zero at the MPP, positive on the left of the MPP and negative on the right of the MPP, as given by Hussein et al. [42]:

$$\frac{dP_{PV}}{dV_{PV}} = 0, at\ MPP.$$
$$\frac{dP_{PV}}{dV_{PV}} > 0, left\ of\ MPP. \qquad (22)$$
$$\frac{dP_{PV}}{dV_{PV}} < 0, right\ of\ MPP.$$

Since:

$$\frac{dP_{PV}}{dV_{PV}} = \frac{d(V_{PV}.I_{PV})}{dV_{PV}} = I_{PV} + V_{PV}.\frac{dI_{PV}}{dV_{PV}} \qquad (23)$$

After measuring the values of V_{PV} and I_{PV} at different instants, the incremental variations, dV_{PV} and dI_{PV}, can be approached by the increments of both parameters ΔV_{PV} and ΔI_{PV} respectively. Therefore, parameters can be given as:

$$dV_{PV} \cong \Delta V_{PV} = V_{PV}(t) - V_{PV}(t - \Delta t) \qquad (24)$$

$$dI_{PV} \cong \Delta I_{PV} = I_{PV}(t) - I_{PV}(t - \Delta t) \qquad (25)$$

$$\frac{dP_{PV}}{dV_{PV}} \cong I_{PV} + V_{PV}.\frac{\Delta I_{PV}}{\Delta V_{PV}} \qquad (26)$$

The basic principle of the incremental conductance method can be rewritten as:

$$\frac{\Delta I_{PV}}{\Delta V_{PV}} = -\frac{I_{PV}}{V_{PV}}, at\ MPP.$$

$$\frac{\Delta I_{PV}}{\Delta V_{PV}} > -\frac{I_{PV}}{V_{PV}}, left\ of\ MPP. \tag{27}$$

$$\frac{\Delta I_{PV}}{\Delta V_{PV}} < -\frac{I_{PV}}{V_{PV}}, right\ of\ MPP.$$

As shown in the flowchart in Figure 19, by comparing the incremental conductance $(\Delta I/\Delta V)$ to the instantaneous conductance (I/V), the MPP can be reached [43]. The PV module is forced to operate at the reference voltage V_{ref}, where at the MPP, $V_{ref} = V_{MPP}$. Once the MPP is captured, the operating point will be stabilized at the MPP unless a change in PV current I_{PV} is noted, implying a change in atmospheric conditions; subsequently, there will be a change in the MPP. In this case, the algorithm decreases or increases the reference voltage V_{ref} with a view to reaching the new MPP [44].
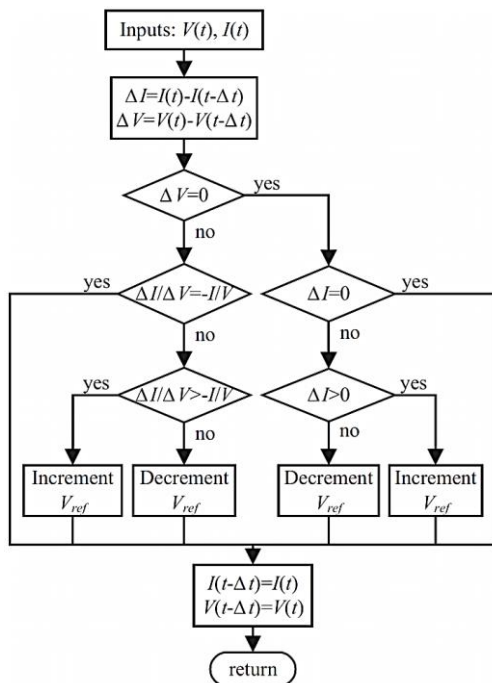
Figure 19. Incremental conductance algorithm flowchart [21].

How fast the MPP can be reached is specified by the increment size. With greater increments, rapid attainment of the MPP can be achieved but the operating point might not be at the MPP exactly and oscillate around it, so there is a tradeoff [45]. Two stages of tracking can be proposed to solve this drawback, in the first stage the operating point is brought near the MPP and then in the second stage the incremental conductance method is employed to track the exact MPP.

2.18 IMPP and VMPP Computation Technique

This technique is based on computing the current and voltage at the MPP, (V_{MPP}, I_{MPP}), from the standard PV current equation, including the irradiance level and ambient temperature. Once calculated, the PV module will be forced to operate at the MPP by using a feedback control loop. Then, the PV array current I_{PV} and voltage V_{PV} at the insolation E and temperature T are given as:

$$I_{PV} = \left[I_S + I_{SC} \left(\frac{E}{E_{STC}} - 1 \right) + \mu(T - T_{STC}) \right].N_P \tag{28}$$

$$V_{PV} = \left[V_S + \beta.(T - T_{STC}) - R_S \left(\frac{1}{N_P} - I_S \right) - \frac{K.I_{PV}}{N_P}(T - T_{STC}) \right].N_S \tag{29}$$

Where I_S & V_S are the output current and voltage of the PV module at the standard test conditions (STC). E_{STC} is the standard solar insolation (1kW/m^2), and T_{STC} is the standard module temperature (25°C). Moreover, I_{SC} is the short circuit current, μ is the temperature coefficient of I_{SC}, β is the temperature coefficient of V_{OC}, R_S is a series resistance of the module and K is the curve correction factor. N_P is the number of parallel-connected modules and N_S is the number of series-connected modules [46].

The output power P_{PV} is calculated as:

$$P_{PV} = V_{PV}.I_{PV} = I_{PV}.\left[V_S + \beta(T - T_{STC}) + R_S.I_S - \frac{I_{PV}}{N_P}.[R_S + K.(T - T_{STC})] \right].N_S \tag{30}$$

The current I_{MPP} and the voltage V_{MPP} at the maximum power point are calculated by differentiating the P_{PV} with respect to the I_{PV}:

$$I_{MPP} = \frac{N_P}{2} \frac{V_S + \beta.(T - T_{STC}) + R_S I_S}{R_S + K(T - T_{STC})} \tag{31}$$

$$V_{MPP} = \frac{N_S}{2}.V_S + \beta.(T - T_{STC}) + R_S.I_S \tag{32}$$

It is notable that the last equations contain the temperature T and do not contain the insolation E. Usually, temperature affects the PV module voltage, and the insolation affects the PV module current. However, the equation of the output power P_{PV} contains the current I_{PV}, and I_{PV} is affected by the insolation E. Therefore, the output power P_{PV} is affected by the insolation E. As a result, even though insolation E does not appear in the equations of the V_{MPP} & I_{MPP}, those equations have effects on insolation E.

As pointed in the equations of the V_{MPP} & I_{MPP}, the maximum power point can be predicted with the module characteristics, and these module characteristics are computed by PV makers. At that time, if there is any difference between the real operating point and the predicted operating point, it indicates that there will be some error in the system. Therefore, this technique can be used for the error diagnosis of the PV system [10]

2.19 Ripple correlation control (RCC)

Once a DC-DC converter is connected to the PV array, the switching action of the power converter forces the current and voltage ripple on the PV array. As a result, the PV array output power will also be submissive to ripple. The MPPT in ripple correlation control is achieved by making use of ripple [47].

In this technique, in order to make the power gradient zero; MPP is reached; the time derivative of the time-varying PV power $\dot{P}_{PV}$ with the time derivative of the time-varying PV voltage $\dot{V}_{PV}$ or current $\dot{I}_{PV}$ is correlated.

If the voltage V_{PV} or the current I_{PV} is increasing $(\dot{V}_{PV} > 0 \ \& \ \dot{I}_{PV} > 0)$ and the power is increasing $(\dot{P}_{PV} > 0)$, then the operating point is beneath the MPP; (on the left side of the P-V curve); $(I < I_{MPP} \ or \ V < V_{MPP})$. On the other side, if the voltage V_{PV} or the current I_{PV} is increasing $(\dot{V}_{PV} > 0 \ \& \ \dot{I}_{PV} > 0)$ and the power is decreasing $(\dot{P}_{PV} < 0)$, then the operating point is over the MPP; (on the right side of the P-V curve); $(I > I_{MPP} \ or \ V > V_{MPP})$. If the power $(\dot{P}_{PV} = 0)$, then the MPP is reached [48].

This method can be achieved by a simple and inexpensive analog circuit. In addition, RCC does not depend on the PV array characteristics, so it can be adapted to different PV systems straightforwardly.

2.20 Fuzzy Logic Control Based MPPT

Over the past decade, the fuzzy logic control method has become common for MPPT since it has many advantages of handling nonlinearity, not requiring an accurate mathematical model, and working with inaccurate inputs [49]. Generally, fuzzy logic control comprises three stages: fuzzification, rule base table lookup, and defuzzification. In the fuzzification stage and based on a membership function, shown in Figure 20, numerical input variables are changed into linguistic variables. In general, five fuzzy levels are used: NB (Negative Big), NS (Negative Small), ZE (Zero), PS (Positive Small), and PB (Positive Big). To increase accuracy, more fuzzy levels can be used [50, 51].
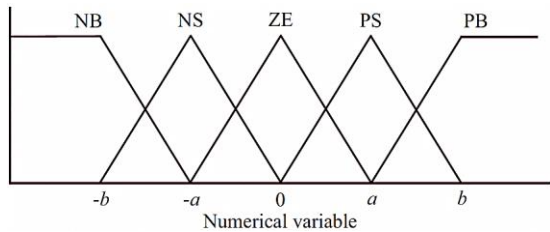

Figure 20. Membership function for inputs and output of fuzzy logic controller [21].

In Figure 20, a and b represent the range of the numerical variable values. Usually, the error E and the change in error ΔE are used as inputs to the MPPT fuzzy logic controller, and the user has the choice of how to compute them.

$$E(n) = \frac{P(n) - P(n-1)}{V(n) - V(n-1)} \tag{33}$$

$$\Delta E = E(n) - E(n-1) \tag{34}$$

After calculating E and ΔE, they will be changed into linguistic variables and the output of the fuzzy logic controller, which is a change in duty cycle ΔD, can be found in the rule base, which is shown in Table 4.

The change in duty cycle ΔD for the various groups of E and ΔE is determined according to the type of power converter being used and the knowledge of the user. From Table 4, for instance, if the operating point is at the far-right end of the MPP, that is the E is NB, and ΔE is ZE, then with a view to reaching the MPP, a large decrease in duty cycle is required, that is ΔD must be NB.

Table 4. The fuzzy logic rule base [21].

ΔE / E	NB	NS	ZE	PS	PB
NB	ZE	ZE	NB	NB	NB
NS	ZE	ZE	NS	NS	NS
ZE	NS	ZE	ZE	ZE	PS
PS	PS	PS	PS	ZE	ZE
PB	PB	PB	PB	ZE	ZE

During the defuzzification stage, the linguistic variables are converted to numerical variables depending on the membership function, as shown in Figure 20. This generates a control signal used to converge the operating point to the MPP.

This method performs well under varying atmospheric conditions. However, its effectiveness is based substantially on the prior experience of the user [51].

2.21 Neural Network Based MPPT

This technique is well adapted for microcontrollers. The neural network typically consists of three layers: input, hidden, and output layers as illustrated in Figure 21. The input variables of the neural network can be the characteristics of the PV module being used or the atmospheric conditions. The output variable is the duty cycle used as a control signal to make the operating point at the MPP. The accuracy of the technique in tracking the MPP relies on the algorithm being used and how well the neural network was trained [52]. The link between nodes i and j is labelled as having a weight of w_{ij}. The more the $w_{ij}'s$ are carefully determined through the training process, the more the MPP can be accurately tracked. In accordance with this, the right weight for every node is obtained by testing and recording the PV parameters over months or years. The disadvantage of this technique is that it needs to be particularly trained for the PV module which is being used. Moreover, the features of the PV module change with time, which means that the neural network should be periodically trained to accurately track the MPP [53].
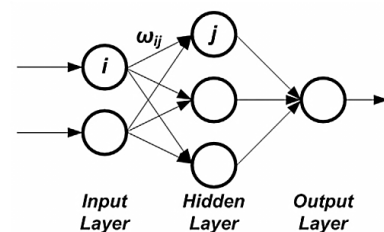

Figure 21. Neural network layers [21].

3 Characteristics During Non-Uniform Irradiance Condition

As is known, the I-V characteristic of a PV panel is directly affected by the change in atmospheric conditions;

in particular, the change of irradiance and temperature. When the PV panel receives a uniform irradiance, the P-V curve exhibits only one MPP which can be captured and tracked by using any one of the conventional MPPT techniques.

Due to many factors such as passing clouds, the shadow cast by the adjacent buildings, trees, bird droppings, dust deposition, etc. the PV panels do not receive uniform irradiance during the daytime. When the solar panel is exposed to partial shading, as shown in Figure 22, the current produced by the shaded cell is lower than the current produced by the unshaded cells, which will lead to negative bias in the shaded cells and instead of generating power will start consuming power leading to a loss in the total output power [54]. The power consumption in the individual shaded cell will lead to overheating which negatively affects surrounding cells. The overheating generates thermal stress on the whole PV panel and hot spot phenomena occurs [55].
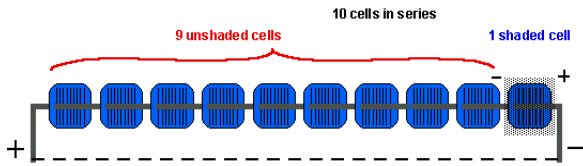

Figure 22. PV string during non-uniform irradiance pattern

To protect the shaded cell from the thermal destruction, (hot spot phenomena) as shown in Figure 23, bypass diodes should be integrated in parallel within the PV panel as shown in Figure 24.

Due to the presence of the bypass diodes, used to block hot spot formation, multiple maximum power points in PV characteristic occurs, as shown in Figure 25 [54].

In this case, conventional MPPT techniques would predominantly not succeed in tracking the appropriate global maximum power point (GMPP) and extra power losses result [56]. For that reason, many new MPPT optimizations have been proposed to address this issue which occurs during partial shading conditions.
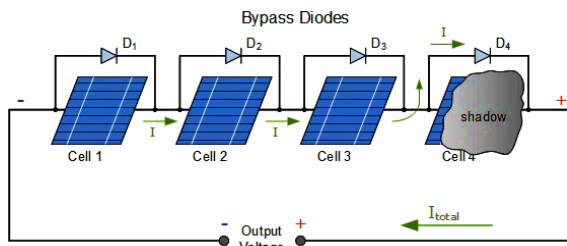

Figure 23. Hot spot phenomena

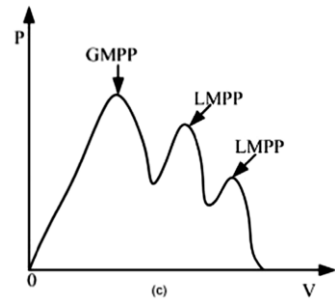**Figure 24.** Bypass diodes connected in parallel within the PV panel [57].

Figure 25. The P-V characteristic under non-uniform irradiance pattern [54].

4 Modern MPPT Optimizations

To overcome the drawbacks of the conventional MPPT techniques and address the PSCs issue, many modern MPPT techniques have been proposed. In this section, the most commonly used techniques are summarized.

4.1 Grey Wolf Optimization

It is inspired by the attack approach used by grey wolves during hunting. This technique has the capability of mimicking the hierarchy leadership as well as the hunting efficiency of grey wolves. With the intention of achieving the effectvie leadership hierarchy, one group of grey wolves is employed, this group contains four kinds of grey wolves; they are alpha (α), beta (β), delta (δ) and omega (ω).

The optimization consists of three procedures; hunting, chasing and tracking of the prey then encircling the prey and attacking it [58, 59]. The hunting mechanism of the grey wolves is led by α clans which are considered leaders and are followed by the β clans. During the hunting process, the wounded wolves are taken care of by the δ and ω clans. This hunting mechanism is employed in the PV system in order to handle the problem of multiple MPPs where the prey represents GMPP in this case. With a view to holding the duty cycle constant at GMPP and reducing steady-state oscillations, the optimization is combined with the direct duty cycle control [60]. The following equations are used to model the hunting technique of grey wolves:

$$\vec{E} = \vec{C}.\overrightarrow{X_P(t)} - \overrightarrow{X_P(t)} \tag{35}$$

$$\overrightarrow{X(t+1)} = \overrightarrow{X_P}(t) - \vec{F}.\vec{E} \tag{36}$$

where, t refers to the present iteration; C, E and F are called the coefficient vectors. The position vector of the prey is symbolized by X_P whereas the position vector for the grey wolf is symbolized by X.

By using the following equations, vectors F and C are calculated:

$$\vec{F} = 2\vec{a}.\overrightarrow{r_1} - \vec{a} \tag{37}$$

$$\vec{C} = 2.\overrightarrow{r_2} \tag{38}$$

The value of a is reduced linearly from 2 to 0, also the vector values of $\vec{r_1} \& \vec{r_2}$ are in [0, 1]. In MPPT applications, the grey wolf represents duty cycle D. Thus, the equation (36) is adjusted as equation (39) and the fitness function of the optimization is calculated by equation (40).

$$D_i(k+1) = D_i(k) - F.E \tag{39}$$

$$P(D_i^k) > P(D_i^{k-1}) \tag{40}$$

where P refers to power; D refers to duty cycle; i represents the number of grey wolves; k denotes the number of iterations. One of the most important advantages of this optimization is eliminating the steady-state oscillations [54].

4.2 Ant Colony Optimizations

This optimization is based on the behavior of ants searching for food [61, 62]. During the food search process, the ants try to find the optimal paths. In this technique, a fitness function f(k) is used to represent the output power, f(k) = I(k) × V(k) and the ants denote the duty cycle. This technique consists of three steps as shown in Figure 26:

1) Initialization and distribution of ants according to the fitness function.
2) Limiting the search interval.
3) Ants move towards the optimal point, the MPP.

After finding the optimal path, the technique provides the proper duty cycle, which is used to drive the DC-DC converter [63, 64].
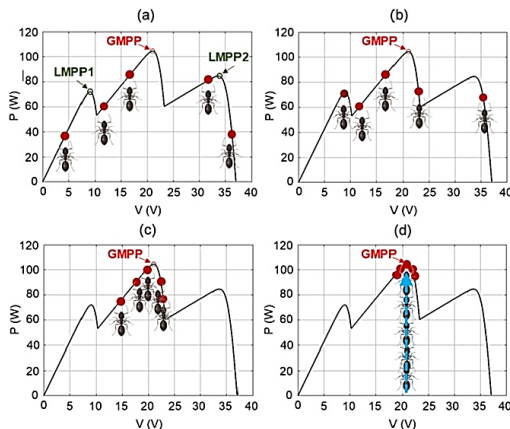

Figure 26. The action steps of the ant colony technique [65].

4.3 Bee Colony Optimization

This technique is considered one of the simplest techniques since it utilizes very few controlled parameters and the initial conditions of the system do not affect the algorithm convergence criteria [66]. It is inspired by the behavior of bees searching for food. As is widely known, the bee colony is divided into three main groups- they are the employed bees, which constantly search the food sources or benefit from the food sources, onlooker bees, which wait in the hive and their role are restricted to making the decisions to choose the food source. The last

group is the scouts, which conduct a random search to find a new food source. In order to get the optimal solution in a short time, the three groups communicate and coordinate together [67, 68]. In MPPT applications, the food position represents the duty cycle, and the food source represents the maximum power. With the aim of implementing this technique in MPPT applications, the duty cycle used to drive the DC-DC converter is calculated as follows:

$$\vec{F} = 2\vec{a}.\vec{r_1} - \vec{a} \tag{41}$$

$$\vec{C} = 2.\vec{r_2} \tag{42}$$

Here, D_e is the current value of duty cycle, D_{min} is the minimum value of duty cycle, D_{max} is the maximum value of duty cycle, $\emptyset_e$ is a constant ranging between (-1, 1) and D_k is the previous value of the duty cycle [68]. The technique was accurate and efficient in finding the GMPP under partial shading conditions.

4.4 Particle Swarm Optimization (PSO)

Among the most popular bio-inspired computation algorithms, PSO is inspired by the social behavior of bird flocking and fish schooling. With different capabilities of reaching optimum solutions, it is good for dealing with problems on which a point or surface represent the best solution [69]. In this algorithm, several cooperative particles are used to conduct the research of the optimal point. If there is available information regarding the location of the GMPP in the search space, the initial position of the particles can be in a fixed position; otherwise, they will be spread in the space randomly. The position of the particle represents the value of the duty cycle [70]. In this algorithm, each particle conducts the search process and collects information, then they exchange the information obtained in their respective search. After that, the particles move toward the optimal point by following the best performing particle. In this way, each particle ultimately evolves to an optimal or close to the optimal solution. Using a large number of particles will increase the accuracy in capturing GMPP; however, that will make the convergence process to the GMPP slow [71, 72]. Although PSO is simple in implementation and able to achieve GMPPT, it is computationally intensive and time-consuming which gradually reduces search accuracy.

4.5 Deterministic Particle Swarm Optimization (DPSO)

To improve the tracking capability and reduce the problem of random searchs, this optimization was modified from conventional particle swarm optimization. In conventional optimization, more iterations will be required to reach the final solution when the change in the duty cycle for two sequential iterations is low. In addition, if the particle is far from the desired point, then a large change in convergence speed is needed, which may make the particle move away from the GMPP. In DPSO, by eliminating the acceleration factor in the convergence speed equation and restricting the convergence speed factor according to the range between two peaks, the

DPSO becomes simpler than the conventional optimization. The optimization has two modes, global mode and local mode. During the partial shading condition, the global mode becomes active. In this case, the algorithm changes into DPSO subroutine, and variable step size perturbation is used during the local mode [72, 73]. The range of duty cycle in global mode is determined as follows:

$$D_{min} = \frac{\sqrt{\eta R_{Lmin}}}{\sqrt{R_{PVmax}} + \sqrt{\eta R_{Lmin}}} \qquad (43)$$

$$D_{max} = \frac{\sqrt{\eta R_{Lmax}}}{\sqrt{R_{PVmin}} + \sqrt{\eta R_{Lmax}}} \qquad (44)$$

where D_{min} & D_{max} denote the minimum and the maximum values of the duty cycle respectively. η refers to the efficiency of the DC-DC converter being used. RL_{min} & RL_{max} denote the minimum and the maximum values of the load. $R_{PV\ min}$ & $R_{PV\ max}$ refer to the reflective impedances of the PV panels [54].

4.6 Switched PV Approach

In this approach, each string in the PV array is equally divided into two parts; the parts are connected together by using two diodes and one controlled switch, as shown in Figure 27.(a). The operating process of this technique has three stages:

1) Stage 1: switches are closed, in this case, the highest output voltage is (V_{OC}) and the highest output current is (n.I_{SC}), where n is the number of parallel-connected strings.
2) Stage 2: switches are opened, in this case, the highest output voltage is ($0.5V_{OC}$) and the highest output current is (2.n.I_{SC}).
3) Stage 3: Selecting the State: MPPT algorithm will activate state1, searches GMPP1. Afterwards, activates state 2, searches for GMPP2 as shown in Figure 27.(b). After that, the MPPT algorithm will compare the values of obtained powers and then decide to switch the system to the state providing increased power [74].
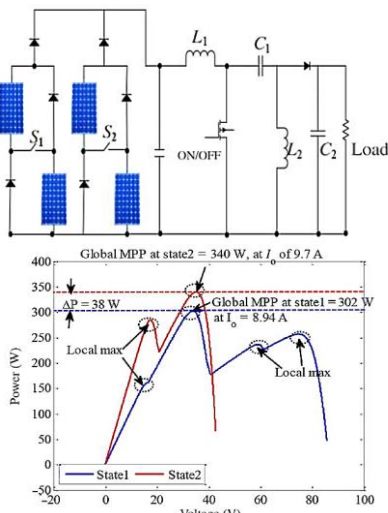

Figure 27. (a) The schematic diagram of the Switched PV technique, (b) Power-voltage characteristic in both states [74].

4.7 A Novel MPPT Method Based on Irradiance Measurement

In the proposed approach, the photodiodes are used as light sensors as shown in Figure 28; the presence of photodiodes gives an innovation feature to this method. The signals provided by the photodiodes allow the algorithm to work properly in spite of the changes in the climatic conditions. The operating process of the proposed method consists of three stages:

1) Detect partial shading.
2) Find the region of the GMPP.
3) Tracking the GMPP by using a conventional technique.

When the photodiodes detect partial shading, the algorithm waits for 30 s to discover whether the shadow is transient or permanent. If the shading continues for more than 30 seconds, the MPPT executes the analysis of the entire PV output curve. Usually, ten points measured along the P–V curve are enough to find the region of the GMPP. Finally, a direct technique, such as P&O, is launched to find and track GMPP [75].
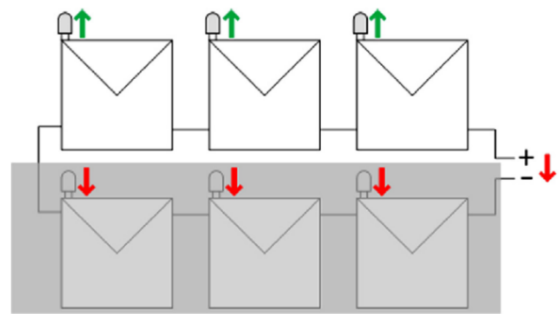

Figure 28. The schematic diagram of the novel MPPT technique [75].

4.8 A Variable Step Size Perturbation & Observation Method

This method is a modified form on conventional P&O and it was proposed to accelerate the convergence to GMPP. In this method, the real MPP is captured and tracked in two modes of operation: the first is the voltage search mode and the second is the MPP search mode. The tracking process used in this method is shown in Figure 29.

During the voltage mode, the operating point of the system is brought near the reference voltage. The reference voltage (V_{ref}) is set at about $0.80*V_{OC}$ to give an approximate location of the real MPP. In the voltage search mode, to increase the convergence speed, the size of the duty cycle is kept large. The size of the duty cycle is gradually reduced as the operating point of the system gets near the reference voltage. When the operating point becomes close to MPP at t1, the MPP search mode becomes activated. The objective of this mode is to bring the operating point as near as possible to the MPP. In this mode, the size of the duty cycle is decreased each time the operating point passes through the MPP. This mode continues until the operating point converges to the MPP at time t2. In this phase, there are two states if the captured

MPP is the GMPP and no other GMPP is available to be captured, a constant and small step size P&O algorithm is activated to start the global tracking. On the other hand, if there is another GMPP, which requires capturing and tracking, the technique switches through the voltage search mode and the MPP search mode to track the other MPPs. This process carries on until all the MPPs are captured one by one. Then the system operates near the real GMPP [76].
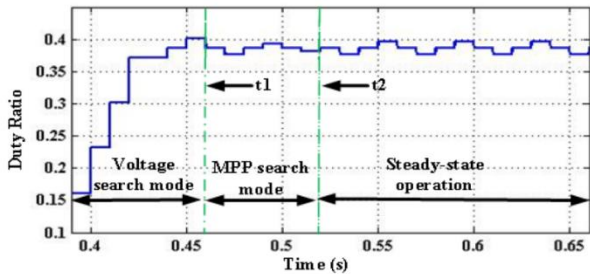

Figure 29. The tracking process in the variable step size P&O technique [76].

4.9 P&O Combined with Particle Swarm Optimization

This technique has two operating stages. In the first stage, in order to conduct a swift search for the first local maximum power point (LMPP), the P&O technique is used. To investigate whether the operating point is going up or down in the P-V characteristic, the operating voltage is perturbed each cycle by a small amount of voltage.

The processing time in the first stage depends on the convergence criterion which must be chosen accurately to determine the first LMPP. If the convergence criterion is large, the algorithm may turn into the second stage before capturing the first LMPP. In contrast, if it is small, a long time may be needed to accomplish the first stage. After reaching the first LMPP, the second stage begins. During this stage, the particle swarm optimization searches for the GMPP. The initial condition of the first particle is chosen according to the value of the convergence voltage in the first stage. For the other particles, the initial conditions range from the convergence voltage to the last point in the search area [77]. The schematic diagram of the proposed system is shown in Figure 30.
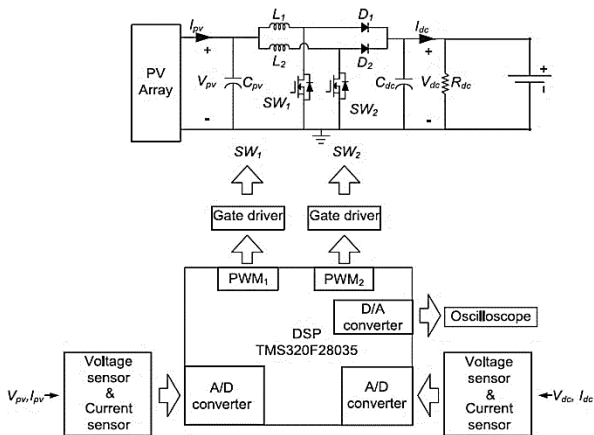

Figure 30. The schematic diagram of the P&O combined with PSO [77].

The most important advantage of this combination that is allows the GMPP to be obtained quickly since the search space is reduced by using the P&O beforehand. In order to improve the efficiency, raise the reliability, and reduce the ripple current; the DC-DC boost converter with an interleaved topology is used.

4.10 A novel technique based on an image of PV modules

The proposed technique relies on estimating the incident irradiance received by the solar panel to calculate the Global Maximum Power Point (GMPP) analytically. This process involves the continuous capture of images of the solar panel using an optical camera, as illustrated in Figure 31. Subsequently, the captured images are input into a mathematical model, as depicted in Figure 32, to determine the incident irradiance. To compute the incident irradiance, the mathematical model takes into account the camera response function and the reflectance characteristics of the solar cells. Once the incident irradiance has been estimated, it becomes possible to calculate the GMPP and its corresponding voltage, relying on the Lambert PV circuits model. To enhance the precision of GMPP calculation and mitigate any inaccuracies stemming from the estimation of incident irradiance, the Perturb and Observe (P&O) technique is employed. This corrective step ensures that external factors such as moisture and dirt, which can adversely impact incident irradiance estimation, do not compromise the accuracy of GMPP determination [78].
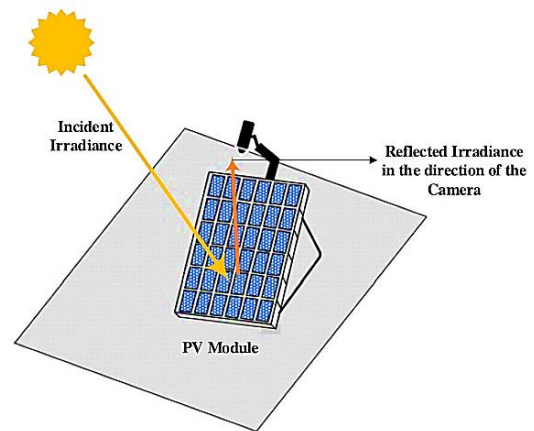
Figure 31. The proposed technique to capture the image of the solar panel [78].
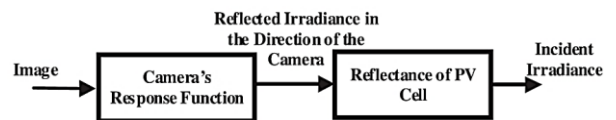
Figure 32. The flowchart for estimating the incident irradiance [78].

4.11 Simulated Annealing Optimization

This optimization is inspired by the metal annealing process. In this optimization, some parameters such as the nominal cooling rate, final temperature rate and initial temperature rate are used to capture the GMPP of the PV system. For every temperature, the optimization measures the corresponding energy to many perturbations it does at

the operating voltage. After that, the measured energy is compared with reference energy. If the measured energy at the new operating point is greater than the reference energy, it is considered as the new operating point. On the other hand, if the measured energy is less than reference energy, it may still be considered based on the acceptance possibility P_r as follows:

$$P_r = \exp\left[\frac{P_k - P_i}{T_k}\right] \tag{45}$$

Here, P_i refers to the power at the previous operating point, P_k refers to the power at the new operating point, and T_k refers to the current system temperature. This optimization consists of two cooling processes, one is adaptive and the other is static kind. The geometric cooling process is expressed as follows:

$$T_K = \alpha T_k - 1 \tag{46}$$

where, T_k refers to the temperature at the current step, $T_k - 1$ refers to the temperature at the previous step and α is a constant ($\alpha < 1$) [79].

4.12 Fuzzy Logic Controller Based on a Single Input

Since the structure of conventional fuzzy logic-based MPPT uses mainly two inputs and has at least 25 rules, it needs a long time for computation and is difficult to be implemented. For these reasons a fuzzy logic controller based on a single input, three rules and three linguistic variables is proposed. In this method, the structure of MPPT is facilitated. According to the P&O technique, the error was taken as $E = (\Delta P/\Delta V)$, for each step, it was concluded that:

If $E < 0$, then $D = D + \Delta D$.

If $E > 0$, then $D = D - \Delta D$.

If $E = 0$, then $D = D$.

In this method, the input signal to the controller is the error E and the output signal of the controller is the change of the duty cycle ΔD. The membership function of the proposed method is shown in Figure 33, where it has three linguistic variables: negative N, positive P and zero ZO. The values of ϕ, r and K are set based on the user experience. The author set them to 4.96, 0.33 and 1, respectively. According to the given membership function, the rules and the linguistic expressions are as follows:

Rule 1: If E is positive mid or positive big, that means the operating point is on the left of the MPP (near or far), then the duty cycle will be negative mid or negative big.
Rule 2: If E is negative mid or negative big, the operating point is on the right of the MPP (near or far), then the duty cycle will be positive mid or positive big.
Rule 3: If E is zero, means the MPP is reached and the change in the duty cycle will be zero.
Once the GMPP is reached, the step of the duty cycle is reduced in order to decrease the steady-state oscillation [80].
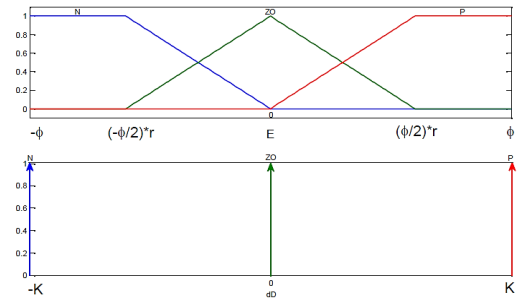

Figure 33. The membership functions of the proposed FLC [80].

4.13 Artificial Neural Network Based MPPT

The proposed technique has two procedures; one becomes active under uniform irradiance conditions, and the other under partial shading conditions. The values of the current and voltage of the PV modules are measured in each sampling time and the difference between the current value of the power and the previous value is calculated. After that, the change in produced power is compared with a preselected threshold value. If the change in the power is less than the certain threshold value, it is considered that the characteristics keep the same shape and the tracking is performed by using one of the conventional MPPT techniques such as P&O or IC. On the other hand, if the threshold value is overflown, which means there is a real change in P-V characteristics, then the ANN-based method is activated to determine the location of GMPP and is followed by one of the conventional methods to perform the tracking. A flowchart of the ANN technique is shown in Figure 34.
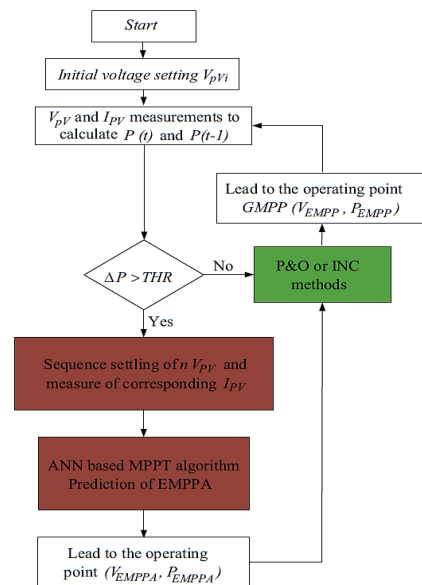
Figure 34. The flowchart of the ANN technique [81].

After activating the ANN method, the power converter, connected between the PV modules and the load, forces the PV modules to sequentially operate at different values of voltage, and then the corresponding current values are measured. The values of current and voltage (I_{PV}, V_{PV}) represent the inputs of the ANN technique. According to the inputs, the ANN provides the value of the voltage corresponding to the GMPP, and then

by the power converter, the operating point is imposed on the PV modules. To improve accuracy, one of the conventional methods is used to make the operating point exactly at the GMPP. In this method, the time needed to predict the GMPP is short and the accuracy is good [81].

4.14 Dormant Particle Swarm Optimization

Since conventional particle swarm optimization (CPSO) uses a random number of particles, it suffers from some drawbacks. First, more iterations are needed by CPSO if the random number of the particles is small; second, if the power values of LMPP and GMPP are close to each other, CPSO may not capture the real GMPP. To overcome these drawbacks, dormant particle swarm optimization (DPSO) is proposed in which the random number of particles is eliminated, and the velocity factor is finite to a certain value. To explain how it functions, let us suppose there are three particles, which are utilized when the PV panels are subjected to partial shading conditions as shown in Figure 35. In CPSO, each particle will search its neighborhood frequently, which means its effect will be limited in a small region leading to an increase in the search time and decrease in efficiency. Nevertheless, in DPSO the process will be as follows:

1) First case: the first particle P1 is near the neighborhood of the second particle P2. In the CPSO, P1 will search frequently the neighbourhood of P2, whereas, in DPSO, this particle will be turned into a dormant state and not participate in the next iteration. Furthermore, the neighborhood of P1 will be dominated by P2.
2) Second case: as shown in Figure 35, since the distance between P2 and P3 is big, P3 will continue sweeping the region between LP3 and LP2.
3) Third case: as has been shown, P2 can catch the GMPP at first since its initial position is near the GMPP. P2 will keep sweeping the region around GMPP during the next iterations.

So in DPSO, the particles have an active state and dormant state. In addition, like the volcano, the dormant particle has an alive state and a dead state. The particle in the first case is in dead dormancy since it will not participate in the next iteration. In contrast, the particles in the second and third cases are in the alive dormancy and they will participate in the next iterations. The DPSO algorithm is combined with the IC algorithm in a dual-algorithm model. After determining the location of GMPP, the IC algorithm is employed to track it accurately [82].
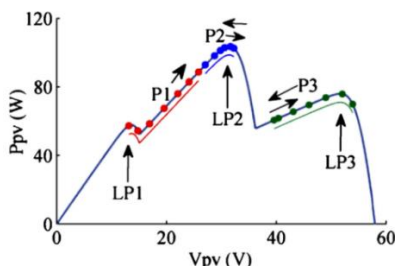

Figure 35. Distribution of particles in PSO [82].

4.15 Genetic Algorithm (GA)

The genetic algorithm (GA) was inspired by natural selection [83]. It is an algorithm based on the concept of survival of the fittest population. Through the iterative use of genetic operators on the existing individuals, the new populations are produced. The main elements of GA are chromosome, selection, crossover, mutation, and fitness functions. The fundamental procedure for GA can be summarized as follows [84]:

1) Defining the input variables which are the population size and the maximum number of iterations.
2) A number of candidate solutions called chromosomes are first evaluated by the fitness function.
3) Choosing a pair of chromosomes from the initial population based on fitness value.
4) Applying the crossover operations on the selected pair with crossover probability.
5) Applying mutation on the offspring with mutation probability.
6) Replacing the old population with the newly generated population.
7) Finding the best global solution.

The working steps of the GA are shown in Figure 36. GA has been used to achieve MPP in many studies. A real-time GA was presented in Ref. [85]. The validity of the proposed method was tested for the identical parameters. It has been found through simulation and experiments that stability can be improved by maximizing a fitness function. The proposed method was effective in finding the GMPP under partial shading conditions and reducing the oscillation around the MPP. However, the GA is complex and requires a long computational time to capture the GMPP.
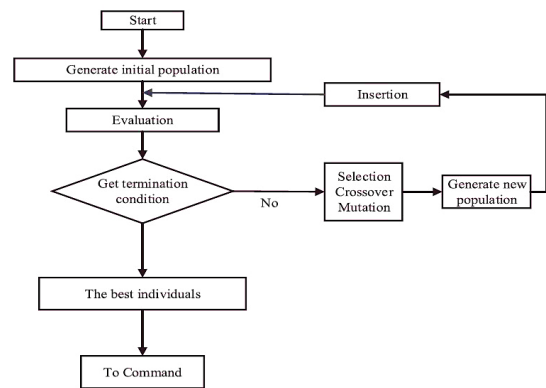
Figure 36. The flowchart of the GA [86].

4.16 Bat Algorithm (BA)

The Bat Algorithm (BA) is a population-based optimization technique bio-inspired on the echolocation features of the microbats in locating their prey [87]. Yang [88] developed the BA by optimizing some of the echolocation characteristics of microbats. This algorithm adopts the features of single microbes in searching and catching prey even in complete darkness [89, 90]. When implementing the main theory of the BA, the following ideas are considered [91]:

1) All bats use their echolocation to feel the distance to their prey. Moreover, they can detect the difference between available foods and physical obstacles.
2) When searching for prey, each bat flies randomly with a constant frequency, loudness, and changing wavelength. Depending on the proximity of the prey, they automatically adjust their wavelength or frequency of the pulse emission rate.
3) With the decreased distance of the prey, the loudness of the bat's changes from a high value to a low fixed value.

In many studies, this algorithm has been employed to address the problems associated with local and global maximum points. Initially, each microbe is given a random frequency value that is distributed between a predefined minimum and maximum value, and once the first-best solution for each microbat is reached in the local search, it proceeds to the second step to find the best new solution. The algorithm conducts a comparison involving all solutions provided by microbats to reach the best global solution [91]. The BA has been used in many studies to deal with PSCs for MPPT applications [92]. Experimental and simulation studies were conducted, and the results showed the efficiency of the algorithm in finding GMPP. The BA was employed to achieve MPP for a Switched Reluctance Motor (SRM) [93]. The optimization was achieved by monitoring the power generated by the solar array and adjusting the duty cycle of the DC-DC converter to obtain the optimum parameters of the control system. The simulation results validated the effectiveness of the proposed method in providing the maximum power of SRM under atmospheric conditions.

4.17 Firefly Algorithm (FA)

This algorithm is based on the firefly phenomenon. The flash produced by the fireflies has many fundamental functions such as mating, hunting and protecting; however, in order to simplify the firefly algorithm (FA), the following assumptions can be made:

1) All fireflies are attracted to each other depending only on brightness and regardless of sex, where the less bright firefly moves to the brighter and more attractive firefly. They will keep moving randomly until they find a brighter one.
2) The objective function affects and determines the level of brightness. Herein, the level of brightness is in direct proportion to the value of the objective function.

In this algorithm, the brightness of the firefly expresses the energy produced from the PV array while the position of the firefly is the duty cycle.

Assuming X_P and X_R are the coordinates for the P & R fireflies, respectively, the distance between them is given as:

$$X_{PR} = \|X_P - X_R\| \tag{47}$$

If the brightness of P is less than the brightness of R, then the firefly P will move towards the firefly R and the new coordinate of P becomes:

$$X_{Pnew} = X_P + \beta.(X_P - X_R) + \alpha.(rand - \tfrac{1}{2}) \tag{48}$$

where β is a function of the distance between two fireflies, rand is a random number uniformly distributed between [0, 1] for each movement of firefly, α is a constant ranging between [0, 1] [94].

The performance of this proposed algorithm is good compared with PSO and P&O algorithms. However, the gradual change in the positions of the fireflies leads to an increase in the convergence time to the GMPP, especially if the number of brighter fireflies is high. This can be explained from Fig. 37. (a), If there are four fireflies and their brightness gradually increases from 1 to 4, then the least bright firefly 1 will first move to firefly 2, then to firefly 3 and later to firefly 4 respectively and the brightness of firefly 1 will change as its position changes. These movements cause an increase in the convergence time to the GMPP. To overcome such a drawback, a modified firefly algorithm (MFA) was proposed [95]. The author suggested that instead of moving the less bright firefly sequentially towards the brighter fireflies, it should move towards the average of the coordinates of all the brighter fireflies as a representative point, as shown in Figure 37. (b). In this case, the final coordinate of the firefly 1 is the average coordinate of the fireflies 2, 3 and 4. It can be formulated as:

$$X_P = X_P + \beta.(X_{javg} - X_P) + \alpha.(rand - \tfrac{1}{2}) \tag{49}$$

Here X_{javg} represents the average coordinates of the brighter fireflies, and is given as:

$$X_{javg} = \tfrac{1}{L}\sum_{m=1}^{L} X_j \tag{50}$$

Here L is the number of the brighter firefly.

Thus, the number of computational operations is reduced resulting in decreasing the time required to converge to GMPP. Although the experimental results showed that MFL has a better performance than FL, the search space will scale up if the GMPP is too far from the initial point.
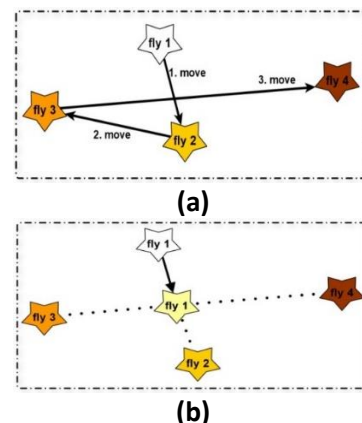

Figure 37. The movement of firefly in: (a) conventional FA; (b) modified FA [96].

4.18 A Hybrid Approach Based on Firefly and P&O Algorithms

With the intention of dealing with the issue of PSCs and improving the convergence speed to GMPP, a hybrid algorithm based on the modified firefly algorithm and the P&O algorithm was proposed [96]. The proposed MPPT technique achieved global tracking by employing three loops. The first loop is called the identifying loop where the location of GMMP is determined. In this loop, seven fireflies are used, and their initial location is manually given. The second loop is called the approximating loop where the operating point of the system is brought near the GMPP. In this loop, the fireflies that produced less power move near the firefly that produced maximum power during the first approximation as shown in Figure 38. Then in the second approximation the fireflies that produced less power in the first approximation, move toward the firefly that produced the maximum power, as shown in Figure 39. At the end of the second loop, one point called a reference point is obtained. From the reference point, the third loop starts tracking the GMPP. In the first and second loops, the Firefly algorithm was used, while the P&O algorithm was used in the third loop. The flowchart of the proposed hybrid algorithm is shown in Figure 40. It is noteworthy that the search range of this algorithm has been reduced which reduced the time required for convergence with the GMPP. Furthermore, the convergence process with GMPP was simplified by manually defining the initial locations of the fireflies. The simulation and experimental results showed the effectiveness and robustness of this algorithm in capturing and tracking the GMPP under different PSCs patterns.
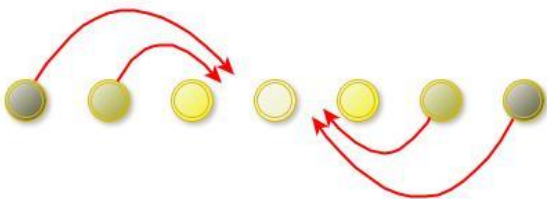

Figure 38. The movement of the fireflies after identifying loop [96].
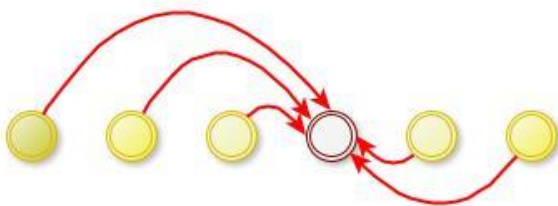

Figure 39. The movement of the fireflies after first approximation [96].

5 Discussion

Research into MPPT techniques to enhance performance is an ongoing endeavor. When evaluating MPPT algorithms and making appropriate selections for a successful design, several criteria must be considered:

1)**Hardware Implementation:** The ease of implementing the proposed algorithm is a crucial factor in selecting the appropriate MPPT technology. Some techniques are straightforward to implement, requiring minimal maintenance and calibration. In contrast, others are more challenging to implement and may necessitate ongoing adjustments to account for changes in surrounding conditions.

2)**Dynamic Response:** Given the rapid changes in climatic conditions that can shift the location of the Maximum Power Point (MPP) on the P-V curve, MPPT algorithms must exhibit a swift response to identify and track the new MPP. This responsiveness is crucial to avoid energy losses.

3)**Sensors Requirement:** Knowledge of input parameters (such as insolation and temperature) and output parameters (voltage and current) of the solar module is essential for MPPT algorithms. Consequently, many MPPT systems employ multiple sensors. However, modified MPPT algorithms often aim to reduce complexity and cost by using fewer sensors.

4)**Tracking Efficiency:** Tracking efficiency is a pivotal characteristic that defines the quality of MPPT algorithms. It is associated with the speed and accuracy of tracking the optimal maximum power point. Tracking efficiency is quantified as the ratio between the actual power extracted from the solar module and the theoretical power under the same atmospheric conditions and during the same period. A well-designed MPPT system should offer high tracking efficiency to improve overall P-V system performance under variable atmospheric conditions.

5)**Cost:** Several factors influence the cost of MPPT systems, including complexity, system features, the number of required sensors, and the difficulty of programming and implementation. Generally, digital systems based on microprocessors tend to be more expensive than analog systems.

In Table 5, a comparison of several conventional and modern MPPT techniques is presented. Notably, the cost was omitted from the comparison due to the challenge of estimating the cost of each technique accurately. However, it's important to note that as the complexity of a technique increases, there is typically a greater reliance on sophisticated systems, which inevitably leads to increased costs.

The ability of the techniques to reliably deal with PSCs was indicated by "no" if it is unreliable and "yes" if it is reliable to converge to the GMPP. The convergence speed is categorized as "fast", "low" and "varies". Here, "varies" means that the convergence to MPP depends on the selection of parameters, for example, the step size of the P&O approach.

The oscillation around MPP is categorized as "no", "yes", "sometimes" and "common". "Sometimes" expresses that the technique may exhibit oscillation around the MPP depending on the implementation and parameter selection, while "common" expresses that the technique often makes oscillation.

The efficiency is indicated as "high", "low", and "varies". It expresses the ability of the technique to reliably track the MPP.

Implementation complexity is categorized as "high", "moderate" and "low". The complexity depends on the need to use sophisticated systems, as well as on the

characteristics of the technique in terms of the implementation difficulty.

Dependence on the characteristics of the PV panels used is shown by "no" or "yes". The case "yes" indicates that initialization is required with the PV panels parameters.

The table shows that there is no single technique that can deal with PSCs while meeting all the required criteria such as simplicity, tracking efficiency, convergence speed, durability, low cost, and others. In general, the weight in choosing the appropriate technique depends on the type of application and the goal to be achieved.
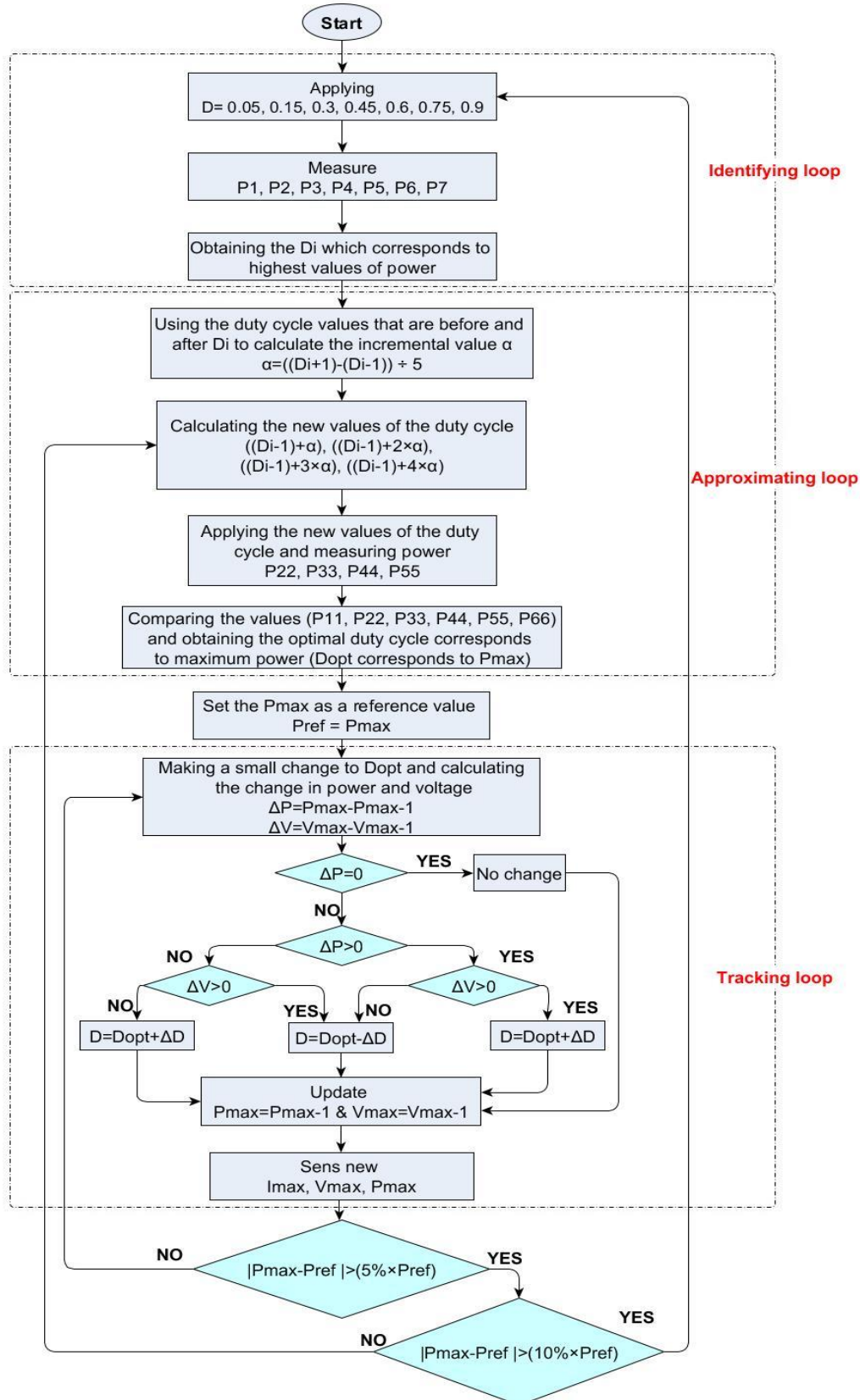

Figure 40. The flowchart of the hybrid approach based on Firefly and P&O algorithms [96].

Table 5. Comprehensive comparison of various conventional and global MPPT techniques

Conventional MPPT techniques							
Technique	Ability to find GMPP	Implementation Complexity	Convergence speed	Efficiency	Sensor requirement	Oscillation around MPP	Dependence on PV panel parameters
Constant voltage (CV)	No	Low	Varies	Low	Voltage	Common	Yes
Open-circuit voltage	No	Low	Fast	Low	Voltage	No	Yes
Short-circuit current	No	Low	Fast	Low	Current	No	Yes
Feedback voltage or current	No	Low	Fast	Low	Voltage or Current	Yes	No
P-N junction drop voltage tracking	No	Low	Varies	Low	Voltage	Yes	Yes
Look-up table	No	Moderate	Varies	Low	Irradiance - Temperature	Common	Yes
Load current or load voltage maximization	No	Low	Varies	Low	Voltage or Current	Yes	No
Only current photovoltaic	No	Low	Varies	Varies	Current	Yes	No
PV output senseless (POS) control	No	Low	Varies	Varies	Current	Yes	No
Perturbation & Observation (P&O)	No	Low	Varies	Varies	Voltage- Current	Common	No
Three-point weight comparison	No	Low	Varies	Varies	Voltage- Current	Sometimes	No
On-line MPP search	No	Moderate	Varies	Varies	Voltage- Current	Common	Yes
DC-link capacitor droop control	No	Low	Low	Varies	Voltage- Current	Common	No
Current sweep	No	Moderate	Low	Low	Voltage- Current	Common	Yes
Incremental conductance (IC)	No	Low	Varies	Varies	Voltage- Current	Common	No
I_{MPP} and V_{MPP} computation	No	Moderate	Varies	Varies	Voltage- Current- Irradiance- Temperature	Common	Yes
Ripple correlation control (RCC)	No	Low	Fast	Varies	Voltage- Current	No	No
Fuzzy logic (FL)	No	High	Fast	Varies	Voltage- Current	No	Yes
Neural network	No	High	Fast	Varies	Irradiance -Voltage- Current	No	Yes
Global MPPT techniques							
Technique	Ability to find GMPP	Implementation Complexity	Convergence speed	Efficiency	Sensor requirement	Oscillation around MPP	Dependence on PV panel characteristics
Grey wolf	Yes	High	Fast	High	Voltage- Current	No	No
Ant colony	Yes	High	Fast	High	Voltage- Current	No	No
Bee colony	Yes	High	Varies	High	Voltage- Current	No	No
Particle swarm (PSO)	Yes	Moderate	Fast	High	Voltage- Current	No	No
Deterministic particle swarm (DPSO)	Yes	High	Fast	High	Voltage- Current	No	No
A variable step size P&O	Yes	Moderate	Fast	Varies	Voltage- Current	Sometimes	Yes
Hybrid P&O and PSO	Yes	High	Fast	High	Voltage- Current	No	No
Simulated annealing (SA)	Yes	High	Fast	High	Voltage- Current- Temperature	Sometimes	No
FL controller based on a single input	Yes	High	Varies	High	Voltage- Current	No	Yes
Artificial neural network (ANN)	Yes	High	Fast	Varies	Voltage- Current	No	Yes
Genetic algorithm (GA)	Yes	High	Varies	Varies	Voltage- Current	No	No
Bat algorithm (BA)	Yes	High	Fast	High	Voltage- Current	No	No
Firefly algorithm (FA)	Yes	Moderate	Fast	High	Voltage- Current	No	No
Hybrid FA and P&O	Yes	Low	Fast	High	Voltage- Current	No	No

Conclusion

This paper has comprehensively reviewed various MPPT algorithms for PV systems, encompassing both conventional and modern techniques. Over the past few decades, many MPPT algorithms have been developed and documented. They exhibit variations in critical aspects such as convergence speed, complexity, cost, required implementation hardware, necessary sensors, and their overall effectiveness.

However, in the pursuit of optimizing PV system performance, it is crucial to adopt a pragmatic approach. If a simpler and more cost-effective algorithm can yield similar or even superior results compared to a more expensive or sophisticated counterpart, it stands to reason that the former should be preferred. This is precisely why

some of the proposed algorithms may not find widespread adoption in real PV system implementations.

Under the challenging conditions of partial shading, conventional MPPT techniques often struggle to accurately track the global maximum power point (GMPP), resulting in significant power losses. In response to this challenge, numerous modern MPPT optimizations have been proposed in the literature. These optimizations demonstrate the ability to capture and track the GMPP effectively. However, it's important to note that many of these modern techniques are constrained by varying degrees of complexity and power dissipation. Furthermore, they rely on intricate computational processes, utilizing artificial intelligence algorithms or soft computing algorithms.

In light of these observations, we hope that the near future will witness the development of high-performance, low-complexity, and cost-effective MPPT techniques. By fully harnessing the output power from PV systems at minimal costs, we can take significant strides towards reducing our dependence on conventional fossil fuel resources.

In conclusion, this study not only provides a comprehensive overview of MPPT techniques for PV systems but also underscores the need for continued research in this field. The pursuit of innovative, efficient, and cost-effective solutions is essential to further the adoption of solar energy and ultimately mitigate our reliance on non-renewable energy sources. This, we believe, will be a vital direction for future research in this domain.

Declaration

Ethics committee approval is not required.

References

[1] Burrett, R., Clini, C., Dixon, R., Eckhart, M., El-Ashry, M., Gupta, D., ... & Ballesteros, A. R. (2009). Renewable energy policy network for the 21st century. *REN21 Renewables Global Status Report.*

[2] Gielen, D., Boshell, F., Saygin, D., Bazilian, M. D., Wagner, N., & Gorini, R. (2019). The role of renewable energy in the global energy transformation. *Energy strategy reviews*, 24, 38-50.

[3] Jalil, M. F., Khatoon, S., Nasiruddin, I., & Bansal, R. C. (2022). Review of PV array modelling, configuration and MPPT techniques. *International Journal of Modelling and Simulation,* 42(4), 533-550.

[4] Worku, M. Y., Hassan, M. A., Maraaba, L. S., Shafiullah, M., Elkadeem, M. R., Hossain, M. I., & Abido, M. A. (2023). A Comprehensive Review of Recent Maximum Power Point Tracking Techniques for Photovoltaic Systems under Partial Shading. *Sustainability*, 15(14), 11132.

[5] Dayaramani, R., Bharadwaj, S. K., & Gawre, S. K. (2017). Simulation and designing of MPPT based solar PV system with DC-DC boost converter. *Simulation*.

[6] Mao, M., Cui, L., Zhang, Q., Guo, K., Zhou, L., & Huang, H. (2020). Classification and summarization of solar photovoltaic MPPT techniques: A review based on traditional and intelligent control strategies. *Energy Reports,* 6, 1312-1327.

[7] Singh, D., & Singh, H. (2019, October). Technical Survey and review on MPPT techniques to attain Maximum Power of Photovoltaic system. *In 2019 5th International Conference on Signal Processing, Computing and Control (ISPCC) (pp. 265-268). IEEE.*

[8] Lasheen, M., Rahman, A. K. A., Abdel-Salam, M., & Ookawara, S. (2016). Performance enhancement of constant voltage based MPPT for photovoltaic applications using genetic algorithm. *Energy Procedia,* 100, 217-222.

[9] Yu, G. J., Jung, Y. S., Choi, J. Y., & Kim, G. S. (2004). A novel two-mode MPPT control algorithm based on comparative study of existing algorithms. *Solar Energy*, 76(4), 455-463.

[10] Karami, N., Moubayed, N., & Outbib, R. (2017). General review and classification of different MPPT Techniques. *Renewable and Sustainable Energy Reviews,* 68, 1-18.

[11] Ngan, M. S., & Tan, C. W. (2011, April). A study of maximum power point tracking algorithms for stand-alone photovoltaic systems. *In 2011 IEEE applied power electronics colloquium (IAPEC) (pp. 22-27). IEEE.*

[12] Shebani, M. M., Iqbal, T., & Quaicoe, J. E. (2016, October). Comparing bisection numerical algorithm with fractional short circuit current and open circuit voltage methods for MPPT photovoltaic systems. *In 2016 IEEE Electrical Power and Energy Conference (EPEC)* (pp. 1-5).

[13] Vâlcan, D. M., Marinescu, C., & Kaplanis, S. (2008, May). Connecting a PV supplied micro-grid to the public grid. *In 2008 11th International Conference on Optimization of Electrical and Electronic Equipment (pp. 369-374).*

[14] Ngan, M. S., & Tan, C. W. (2011, April). A study of maximum power point tracking algorithms for stand-alone photovoltaic systems. *In 2011 IEEE applied power electronics colloquium (IAPEC) (pp. 22-27).*

[15] Oh, T., Hassan, O., Shamsir, S., & Islam, S. K. (2019, June). DC-DC boost converter design with maximum power point tracker (MPPT) used in RF-energy harvester. *In 2019 IEEE International Symposium on Medical Measurements and Applications (MeMeA)* (pp. 1-5).

[16] Baimel, D., Shkoury, R., Elbaz, L., Tapuchi, S., & Baimel, N. (2016, June). Novel optimized method for maximum power point tracking in PV systems using Fractional Open Circuit Voltage technique. *In 2016 International Symposium on Power Electronics, Electrical Drives, Automation and Motion (SPEEDAM) (pp. 889-894).* IEEE.

[17] Hui, J. C., Bakhshai, A., & Jain, P. K. (2015). A sensorless adaptive maximum power point extraction method with voltage feedback control for small wind turbines in off-grid applications. *IEEE Journal of Emerging and Selected Topics in Power Electronics, 3(3), 817-828.*

[18] Kobayashi, K., Matsuo, H., & Sekine, Y. (2006). An excellent operating point tracker of the solar-cell power supply system. *IEEE Transactions on Industrial Electronics*, 53(2), 495-499.

[19] Kim, Y., Jo, H., & Kim, D. (1996, August). A new peak power tracker for cost-effective photovoltaic power system. In IECEC 96. *Proceedings of the 31st Intersociety Energy Conversion Engineering Conference* (Vol. 3, pp. 1673-1678). IEEE.

[20] Kota, V. R., & Bhukya, M. N. (2016, February). A simple and efficient MPPT scheme for PV module using 2-dimensional lookup table. *In 2016 IEEE Power and Energy Conference at Illinois (PECI) (pp. 1-7).* IEEE.

[21] Esram, T., & Chapman, P. L. (2007). Comparison of photovoltaic array maximum power point tracking techniques. *IEEE Transactions on energy conversion*, 22(2), 439-449.

[22] Kislovski, A. S., & Redl, R. (1994, June). Maximum-power-tracking using positive feedback. *In Proceedings of 1994 Power Electronics Specialist Conference-PESC'94* (Vol. 2, pp. 1065-1068). IEEE.

[23] Salas, V., Olias, E., Lazaro, A., & Barrado, A. (2005). New algorithm using only one variable measurement applied to a maximum power point tracker. *Solar energy materials and solar cells,* 87(1-4), 675-684.

[24] Salas, V. O. E. L. A., Olias, E., Lazaro, A., & Barrado, A. (2005). Evaluation of a new maximum power point tracker (MPPT) applied to the photovoltaic stand-alone systems. Solar energy materials and solar cells, 87(1-4), 807-815.

[25] S.-J. Lee et al., "The experimental analysis of the grid-connected PV system applied by POS MPPT," *in 2007 International Conference on Electrical Machines and Systems* (ICEMS), 2007: IEEE, pp. 1786-1791.

[26] Kim, S. Y., Park, S., Jang, S. J., Kim, G. H., Seo, H. R., Park, M., & Yu, I. K. (2009, November). An effective POS MPPT control method for PV power generation system. *In 2009 International Conference on Electrical Machines and Systems (pp. 1-6).* IEEE.

[27] Mohammed, S. S., Devaraj, D., & Ahamed, T. I. (2016). A novel hybrid maximum power point tracking technique using perturb & observe algorithm and learning automata for solar PV system. *Energy*, 112, 1096-1106.

[28] Omar, F. A., Gökküş, G., & Kulaksız, a. A. (2019). Şebekeden Bağımsız FV Sistemde Maksimum Güç Noktası Takip Algoritmalarının Değişken Hava Şartları Altında Karşılaştırmalı Analizi. *Konya Journal of Engineering Sciences,* 7(3), 585-594.

[29] Motahhir, S., El Hammoumi, A., & El Ghzizal, A. (2018). Photovoltaic system with quantitative comparative between an improved MPPT and existing INC and P&O methods under fast varying of solar irradiation. *Energy Reports*, 4, 341-350.

[30] Roy, C. P., Naick, B. K., & Shankar, G. (2013). Modified three-point weight comparison method for adaptive MPPT of photovoltaic systems. In *Fifth International Conference on Advances in Recent Technologies in Communication and Computing (ARTCom 2013)* (s. 146-156).

[31] Hsiao, T., & Chen, C. H. (2002). Maximum power tracking for photovoltaic power system. *In Conference Record of the 2002 IEEE Industry Applications Conference.* 37th IAS Annual Meeting (s. 1035-1040). IEEE.

[32] Altas, I. H., & Sharaf, A. M. (1996). A novel on-line MPP search algorithm for PV arrays. *IEEE Transactions on Energy Conversion,* 11(4), 748-754.

[33] Altas, I., & Sharaf, A. (1996). A novel on-line MPP search algorithm for PV arrays. *IEEE Transactions on Energy Conversion*, 11(4), 748-754.

[34] Godoy, R. B., Bizarro, D. B., De Andrade, E. T., de Oliveira Soares, J., Ribeiro, P. E. M. J., Carniato, L. A., ... & Canesin, C. A. (2016). Procedure to match the dynamic response of MPPT and droop-controlled microinverters. *IEEE transactions on industry applications,* 53(3), 2358-2368.

[35] Matsui, M., Kitano, T., Xu, D.-h., & Yang, Z.-q. (1999). A new maximum photovoltaic power tracking control scheme based on power equilibrium at DC link. In Conference Record of the 1999 IEEE Industry Applications Conference. *Thirty-Forth IAS Annual Meeting* (s. 804-809). IEEE.

[36] Kitano, T., Matsui, M., & Xu, D.-h. (2001). Power sensor-less MPPT control scheme utilizing power balance at DC link-system design to ensure stability and response. *In IECON'01. 27th Annual Conference of the IEEE Industrial Electronics Society* (s. 1309-1314). IEEE.

[37] Zhang, L., Hurley, W. G., & Wölfle, W. H. (2011). A New Approach to Achieve Maximum Power Point Tracking for PV System With a Variable Inductor. *IEEE Transactions on Power Electronics, 26(4),* 1031-1037.

[38] Zhang, L., Hurley, W. G., & Wölfle, W. H. (2010). A new approach to achieve maximum power point tracking for PV system with a variable inductor. *IEEE Transactions on Power Electronics,* 26(4), 1031-1037.

[39] Husain, M. A., et al. (2017). Comparative assessment of maximum power point tracking procedures for photovoltaic systems. *Green Energy & Environment*, 2(1), 5-17.

[40] Bodur, M., & Ermis, M. (1994). Maximum power point tracking for low power photovoltaic solar panels. In Proceedings of MELECON'94. *Mediterranean Electrotechnical Conference (s. 758-761).* IEEE.

[41] AlhajOmar, F., Gokkus, G., & Kulaksiz, A. A. (2019). Rapid Control Prototyping Based on 32-bit ARM Cortex-M3 Microcontroller for Photovoltaic MPPT Algorithms. *International Journal of Renewable Energy Research*, 9.

[42] Hussein, K., Muta, I., Hoshino, T., & Osakada, M. (1995). Maximum photovoltaic power tracking: an algorithm for rapidly changing atmospheric conditions. *IEE Proceedings-Generation, Transmission Distribution,* 142(1), 59-64.

[43] Anwer, A. M. O., Omar, F. A., Bakir, H., & Kulaksiz, A. A. (2020). Sensorless Control of a PMSM Drive Using EKF for Wide Speed Range Supplied by MPPT Based Solar PV System. *Elektronika ir Elektrotechnika*, 26(1), 32-39.

[44] Salas, V., Olias, E., Barrado, A., & Lazaro, A. (2006). Review of the maximum power point tracking algorithms for stand-alone photovoltaic systems. *Solar Energy Materials and Solar Cells,* 90(11), 1555-1578.

[45] Anowar, M. H., & Roy, P. (2019). A Modified Incremental Conductance Based Photovoltaic MPPT Charge Controller. *In 2019 International Conference on Electrical, Computer and Communication Engineering (ECCE) (pp. 1-5).*

[46] Takashima, T., Tanaka, T., Amano, M., & Ando, Y. (2000). Maximum output control of photovoltaic (PV) array. *In Collection of Technical Papers. 35th Intersociety Energy Conversion Engineering Conference and Exhibit (IECEC)* (Vol. 1, pp. 380-383). IEEE.

[47] Rafiei, M., Abdolmaleki, M., & Mehrabi, A. H. (2012). A new method of maximum power point tracking (MPPT) of photovoltaic (PV) cells using impedance adaption by Ripple correlation control (RCC). *In 2012 Proceedings of 17th Conference on Electrical Power Distribution*, 2-3 May 2012 (pp. 1-8).

[48] Midya, P., Krein, P. T., Turnbull, R. J., Reppa, R., & Kimball, J. (1996). Dynamic maximum power point tracker for photovoltaic applications. *In PESC Record. 27th Annual IEEE Power Electronics Specialists Conference* (Vol. 2, pp. 1710-1716).

[49] Bendib, B., Krim, F., Belmili, H., Almi, M. F., & Boulouma, S. (2014). Advanced Fuzzy MPPT Controller for a Stand-alone PV System. *Energy Procedia, 50,* 383-392.

[50] Anwer, A. M. O., Omar, F. A., & Kulaksiz, A. A. (2020). Design of a Fuzzy Logic-based MPPT Controller for a PV System Em-ploying Sensorless Control of MRAS-based PMSM. *International Journal of Control Automation Systems.*

[51] Kottas, T. L., Boutalis, Y. S., & Karlis, A. D. (2006). New maximum power point tracker for PV arrays using fuzzy controller in close cooperation with fuzzy cognitive networks. *IEEE Transactions on Energy Conversion*, 21(3), 793-803.

[52] Liu, Y.-H., Liu, C.-L., Huang, J.-W., & Chen, J.-H. (2013). Neural-network-based maximum power point tracking methods for photovoltaic systems operating under fast changing environments. *Solar Energy*, 89, 42-53.

[53] Hiyama, T., Kouzuma, S., & Imakubo, T. (1995). Identification of optimal operating point of PV modules using neural network for real time maximum power tracking control. *IEEE Transactions on Energy Conversion*, 10(2), 360-367.

[54] Mohapatra, A., Nayak, B., Das, P., & Mohanty, K. B. (2017). A review on MPPT techniques of PV system under partial shading condition. *Renewable Sustainable Energy Reviews,* 80, 854-867.

[55] Gosumbonggot, J., & Fujita, G. (2019). Photovoltaic's Hotspot and Partial Shading Detection Algorithm Using Characteristic Curve's Analysis. *In 2019 9th International Conference on Power and Energy Systems (ICPES)* (pp. 1-6).

[56] Omar, F. A., Pamuk, N., & Kulaksız, A. A. (2023). A critical evaluation of maximum power point tracking techniques for PV systems working under partial shading conditions. *Turkish Journal of Engineering*, 7(1), 73-81.

[57] Chaudhary, A., Gupta, S., Pande, D., Mahfooz, F., & Varshney, G. (2015). Effect of partial shading on characteristics of PV panel using Simscape. *International Journal of Engineering Research and Applications,* 5(10), 85-89.

[58] Laxman, B., Annamraju, A., & Srikanth, N. V. (2021). A grey wolf optimized fuzzy logic based MPPT for shaded solar photovoltaic systems in microgrids. *International Journal of Hydrogen Energy,* 46(4), 3182-3193.

[59] Pamuk, N. (2023). Performance Analysis of Different Optimization Algorithms for MPPT Control Techniques under Complex Partial Shading Conditions in PV Systems. *Energies,* 16(8), 3358.

[60] Mohanty, S., Subudhi, B., & Ray, P. K. (2015). A new MPPT design using grey wolf optimization technique for photovoltaic system under partial shading conditions. *IEEE Transactions on Sustainable Energy,* 6(1), 181-188.

[61] Phanden, R. K., Sharma, L., Chhabra, J., & İ. Demir, H. (2020). A novel modified ant colony optimization based maximum power point tracking controller for photovoltaic systems. *Materials Today: Proceedings*.

[62] Huang, K.-H., Chao, K.-H., & Lee, T.-W. (2023). An Improved Photovoltaic Module Array Global Maximum Power Tracker Combining a Genetic Algorithm and Ant Colony Optimization. *Technologies,* 11(2), 61.

[63] Jiang, L. L., Maskell, D. L., & Patra, J. C. (2013). A novel ant colony optimization-based maximum power tracking for photovoltaic systems under partially shaded conditions. *Energy Buildings,* 58, 227-236.

[64] Jiang, L. L., & Maskell, D. L. (2014). A uniform implementation scheme for evolutionary optimization algorithms and the experimental implementation of an ACO based MPPT for PV systems under partial shading. *In 2014 IEEE Symposium on Computational Intelligence Applications in Smart Grid (CIASG)* (pp. 1-8). IEEE.

[65] Motahhir, S., El Hammoumi, A., & El Ghzizal, A. (2020). The most used MPPT algorithms: Review and the suitable low-cost embedded board for each algorithm. *Journal of cleaner production,* 246, 118983.

[66] Fanani, M. R., Sudiharto, I., & Ferdiansyah, I. (2020). Implementation of Maximum Power Point Tracking on PV System using Artificial Bee Colony Algorithm. *In 2020 3rd International Seminar on Research of Information Technology and Intelligent Systems (ISRITI)* (pp. 117-122).

[67] Sundareswaran, K., Sankar, P., Nayak, P. S. R., Simon, S. P., & Palani, S. (2014). Enhanced energy output from a PV system under partial shaded conditions through artificial bee colony. *IEEE transactions on sustainable energy*, 6(1), 198-209.

[68] Benyoucef, A. S., Chouder, A., Kara, K., & Silvestre, S. (2015). Artificial bee colony based algorithm for maximum power point tracking (MPPT) for PV systems operating under partial shaded conditions. *Applied Soft Computing*, 32, 38-48.

[69] Wasim, M. S., Amjad, M., Habib, S., Abbasi, M. A., Bhatti, A. R., & Muyeen, S. (2022). A critical review and performance comparisons of swarm-based optimization algorithms in maximum power point tracking of photovoltaic systems under partial shading conditions. *Energy Reports,* 8, 4871-4898.

[70] Wei-Ru, C., Chen, L., Chia-Hsuan, W., & Ci-Min, L. (2015). Multicluster-based particle swarm optimization algorithm for photovoltaic maximum power point tracking. *In 2015 IEEE 2nd International Future Energy Electronics Conference (IFEEC)* (pp. 1-6).

[71] Liu, Y.-H., Huang, S.-C., Huang, J.-W., & Liang, W.-C. (2012). A particle swarm optimization-based maximum power point tracking algorithm for PV systems operating under partially shaded conditions. *IEEE Transactions on Energy Conversion,* 27(4), 1027-1035.

[72] Ishaque, K., Salam, Z., Taheri, H., & Shamsudin, A. (2011). Maximum power point tracking for PV system under partial shading condition via particle swarm optimization. *In 2011 IEEE Applied Power Electronics Colloquium (IAPEC)* (pp. 5-9).

[73] Ishaque, K., Salam, Z., Amjad, M., & Mekhilef, S. (2012). An improved particle swarm optimization (PSO)–based MPPT for PV with reduced steady-state oscillation. *IEEE transactions on Power Electronics, 27(8),* 3627-3638.

[74] Elserougi, A. A., Diab, M. S., Massoud, A. M., Abdel-Khalik, A. S., & Ahmed, S. (2015). A switched PV approach for extracted maximum power enhancement of PV arrays during partial shading. *IEEE Transactions on Sustainable Energy, 6(3),* 767-772.

[75] Bayod-Rújula, Á.-A., & Cebollero-Abián, J.-A. (2014). A novel MPPT method for PV systems with irradiance measurement. *Solar Energy*, 109, 95-104.

[76] Ahmad, J., Spertino, F., Di Leo, P., & Ciocia, A. (2016). A variable step size perturb and observe method based MPPT for partially shaded photovoltaic arrays. *In PCIM Europe 2016; International Exhibition and Conference for Power Electronics, Intelligent Motion, Renewable Energy and Energy Management* (pp. 1-8).

[77] Lian, K., Jhang, J., & Tian, I. (2014). A maximum power point tracking method based on perturb-and-observe combined with particle swarm optimization. *IEEE journal of photovoltaics,* 4(2), 626-633.

[78] Mahmoud, Y., & El-Saadany, E. F. (2016). A novel MPPT technique based on an image of PV modules. *IEEE Transactions on Energy Conversion,* 32(1), 213-221.

[79] Lyden, S., & Haque, M. E. (2015). A simulated annealing global maximum power point tracking approach for PV modules under partial shading conditions. *IEEE Transactions on Power Electronics,* 31(6), 4171-4181.

[80] Benlahbib, B., Bouarroudj, N., Mekhilef, S., Abdelkrim, T., Lakhdari, A., & Bouchafaa, F. J. E. i. E. (2018). A Fuzzy Logic Controller Based on Maximum Power Point Tracking Algorithm for Partially Shaded PV Array-Experimental Validation. *Elektronika ir Elektrotechnika,* 24(4), 38-44.

[81] Rizzo, S. A., & Scelba, G. (2015). ANN based MPPT method for rapidly variable shading conditions. *Applied Energy,* 145, 124-132.

[82] Shi, J., Zhang, W., Zhang, Y., Xue, F., & Yang, T. (2015). MPPT for PV systems based on a dormant PSO algorithm. *Electric Power Systems Research,* 123, 100-107.

[83] Chao, K.-H., & Rizal, M. N. (2021). A Hybrid MPPT Controller Based on the Genetic Algorithm and Ant Colony Optimization for Photovoltaic Systems under Partially Shaded Conditions. *Energies*, 14(10), 2902.

[84] Katoch, S., Chauhan, S. S., & Kumar, V. (2021). A review on genetic algorithm: past, present, and future. *Multimedia tools and applications*, 80, 8091-8126.

[85] Hadji, S., Gaubert, J.-P., & Krim, F. (2018). Real-Time Genetic Algorithms-Based MPPT: Study and Comparison (Theoretical an Experimental) with Conventional Methods. *Energies*, 11(2), 459.

[86] Baba, A. O., Liu, G., & Chen, X. (2020). Classification and evaluation review of maximum power point tracking methods. *Sustainable Futures*, 2, 100020.

[87] Asim, M., Agrawal, P., Tariq, M., & Alamri, B. (2021). MPPT-based on Bat algorithm for photovoltaic systems working under partial shading conditions. *Journal of Intelligent & Fuzzy Systems*, Preprint, 1-9.

[88] Yang, X.-S. (2010). A new metaheuristic bat-inspired algorithm. *In Nature inspired cooperative strategies for optimization (NICSO 2010).* Springer, pp. 65-74.

[89] Kaced, K., Larbes, C., Ramzan, N., Bounabi, M., & Dahmane, Z. e. (2017). Bat algorithm based maximum power point tracking for photovoltaic system under partial shading conditions. *Solar Energy,* 158, 490-503.

[90] Wu, Z., & Yu, D. (2018). Application of improved bat algorithm for solar PV maximum power point tracking under partially shaded condition. *Applied Soft Computing*, 62, 101-109.

[91] Da Rocha, M. V., Sampaio, L. P., & da Silva, S. A. O. (2020). Comparative analysis of MPPT algorithms based on Bat algorithm for PV systems under partial shading condition. *Sustainable Energy Technologies and Assessments,* 40, 100761.

[92] Eltamaly, A. M. (2021). Optimal control parameters for bat algorithm in maximum power point tracker of photovoltaic energy systems. *International Transactions on Electrical Energy Systems,* 31(4), e12839.

[93] Oshaba, A. S., Ali, E. S., & Abd Elazim, S. M. (2015). MPPT control design of PV system supplied SRM using BAT search algorithm. *Sustainable Energy, Grids and Networks,* 2, 51-60.

[94] Sundareswaran, K., Peddapati, S., & Palani, S. (2014). MPPT of PV systems under partial shaded conditions through a colony of flashing fireflies. *IEEE Transactions on Energy Conversion,* 29(2), 463-472.

[95] Teshome, D., Lee, C., Lin, Y., & Lian, K. (2016). A modified firefly algorithm for photovoltaic maximum power point tracking control under partial shading. *IEEE Journal of Emerging Selected Topics in Power Electronics,* 5(2), 661-671.

[96] Alhaj Omar, F., & Kulaksiz, A. A. (2021). Experimental evaluation of a hybrid global maximum power tracking algorithm based on modified firefly and perturbation and observation algorithms. *Neural Computing and Applications,* 33(24), 17185-17208.